Human CD1c$^+$ Myeloid Dendritic Cells Acquire a High Level of Retinoic Acid–Producing Capacity in Response to Vitamin D_3

Takayuki Sato,*,† Toshio Kitawaki,* Haruyuki Fujita,* Makoto Iwata,†,‡ Tomonori Iyoda,†,§ Kayo Inaba,†,§ Toshiaki Ohteki,†,¶ Suguru Hasegawa,‖ Kenji Kawada,‖ Yoshiharu Sakai,‖ Hiroki Ikeuchi,# Hiroshi Nakase,** Akira Niwa,††,‡‡ Akifumi Takaori-Kondo,* and Norimitsu Kadowaki*,†

All-*trans*-retinoic acid (RA) plays a critical role in maintaining immune homeostasis. Mouse intestinal CD103$^+$ dendritic cells (DCs) produce a high level of RA by highly expressing retinal dehydrogenase (RALDH)2, an enzyme that converts retinal to RA, and induce gut-homing T cells. However, it has not been identified which subset of human DCs produce a high level of RA. In this study, we show that CD1c$^+$ blood myeloid DCs (mDCs) but not CD141^{high} mDCs or plasmacytoid DCs exhibited a high level of RALDH2 mRNA and aldehyde dehydrogenase (ALDH) activity in an RA- and p38-dependent manner when stimulated with 1α,25-dihydroxyvitamin D_3 (VD_3) in the presence of GM-CSF. The ALDH activity was abrogated by TLR ligands or TNF. CD103$^-$ rather than CD103$^+$ human mesenteric lymph node mDCs gained ALDH activity in response to VD_3. Furthermore, unlike in humans, mouse conventional DCs in the spleen and mesenteric lymph nodes gained ALDH activity in response to GM-CSF alone. RALDH2^{high} CD1c$^+$ mDCs stimulated naive CD4$^+$ T cells to express gut-homing molecules and to produce Th2 cytokines in an RA-dependent manner. This study suggests that CD1c$^+$ mDCs are a major human DC subset that produces RA in response to VD_3 in the steady state. The "vitamin D – CD1c$^+$ mDC – RA" axis may constitute an important immune component for maintaining tissue homeostasis in humans. *The Journal of Immunology*, **2013, 191: 3152–3160.**

Dendritic cells (DCs) play a pivotal role in controlling immune responses in terms of their magnitude and quality, such as immunity versus tolerance, depending on the tissue milieu. This eventually leads to maintaining immune homeostasis by eliminating pathogens and by avoiding harmful inflammation. Recent studies using mice revealed the importance of all-*trans*-retinoic acid (hereafter referred to as RA) derived from DCs in maintaining immune homeostasis in the intestine (1) and possibly in other organs (2). It has been shown that CD103$^+$ DCs in lamina propria and mesenteric lymph nodes (MLNs) produce RA and thus to promote the generation of gut-homing regulatory T (Treg) cells (3). GM-CSF (4) and RA (4–8) are pivotal factors to induce mouse DCs to express retinal dehydrogenase (RALDH)2, which is encoded by the aldehyde dehydrogenase 1 family, member A2 (*ALDH1A2*) gene and converts retinal to RA. IL-4 (4, 9) and TLR ligands (2, 4, 5, 10–12) augment the expression of RALDH2. These studies have presented a model that appropriately stimulated CD103$^+$ DCs in gut-associated tissues produce RA and thus induce gut-homing Treg cells, resulting in maintaining immune homeostasis in the intestine in mice. Surprisingly, however, human DCs that express a high level of RALDH have not been identified.

Human DC subsets in blood and lymphoid tissues are composed of myeloid DCs (mDCs) and plasmacytoid DCs (pDCs) (13). mDCs are further subdivided into CD141 (BDCA-3)^{high} mDCs and CD1c (BDCA-1)$^+$ mDCs, and the former corresponds to mouse CD8$^+$ CD11b$^-$ conventional DCs (cDCs) in lymphoid tissues (14–16) and CD103$^+$ cDCs in nonlymphoid tissues (17) that efficiently cross-present Ags. In contrast, distinctive functions of the latter, which is likely equivalent to mouse CD8$^-$CD11b$^+$ cDCs (18), have been elusive. In addition, monocytes and CD34$^+$ hematopoietic progenitors can differentiate into DCs in the presence of appropriate cytokine mixtures. However, it remains unclear which DCs in situ correspond to DCs induced in vitro from monocytes or CD34$^+$ progenitors. Therefore, it is important to obtain data using DCs isolated from blood and tissues to gain an insight into physiological and clinical relevance of basic researches on human DCs.

*Department of Hematology and Oncology, Graduate School of Medicine, Kyoto University, Kyoto 606-8507, Japan; †Japan Science and Technology Agency, Core Research for Evolutional Science and Technology, Tokyo 102-0076, Japan; ‡Laboratory of Immunology, Kagawa School of Pharmaceutical Sciences, Tokushima Bunri University, Kagawa 769-2193, Japan; §Division of Systemic Life Science, Department of Animal Development and Physiology, Laboratory of Immunology, Graduate School of Biostudies, Kyoto University, Kyoto 606-8501, Japan; ¶Department of Biodefense Research, Medical Research Institute, Tokyo Medical and Dental University, Tokyo 101-0062, Japan; ‖Department of Surgery, Graduate School of Medicine, Kyoto University, Kyoto 606-8507, Japan; #Department of Surgery, Hyogo College of Medicine, Hyogo 663-8501, Japan; **Department of Gastroenterology and Hepatology, Graduate School of Medicine, Kyoto University, Kyoto 606-8507, Japan; ††Department of Pediatrics, Graduate School of Medicine, Kyoto University, Kyoto 606-8507, Japan; and ‡‡Department of Clinical Application, Center for iPS Cell Research and Application, Kyoto University, Kyoto 606-8507, Japan

Received for publication December 26, 2012. Accepted for publication July 16, 2013.

This work was supported by research funding from the Japan Science and Technology Agency, Core Research for Evolutional Science and Technology (to N.K.).

Address correspondence and reprint requests to Dr. Norimitsu Kadowaki, Department of Hematology and Oncology, Graduate School of Medicine, Kyoto University, 54 Shogoin Kawahara-cho, Sakyo-ku, Kyoto 606-8507, Japan. E-mail address: kadowaki@kuhp.kyoto-u.ac.jp

The online version of this article contains supplemental material.

Abbreviations used in this article: ALDH, aldehyde dehydrogenase; ALDH1A2, aldehyde dehydrogenase 1 family, member A2; cDC, conventional dendritic cell; CLA, cutaneous lymphocyte Ag; DC, dendritic cell; DEAB, diethylaminobenzaldehyde; GUSB, β-glucuronidase; mDC, myeloid DC; MFI, mean fluorescence intensity; MLN, mesenteric lymph node; MoDC, monocyte-derived DC; pDC, plasmacytoid DC; PE-Cy5, PE-Cyanin 5; RA, all-*trans*-retinoic acid; RALDH, retinal dehydrogenase; RAR, pan-RA receptor; rh, recombinant human; Treg, regulatory T; VD_3, 1α,25-dihydroxyvitamin D_3; VDR, vitamin D receptor.

www.jimmunol.org/cgi/doi/10.4049/jimmunol.1203517

In the current study, we used human DCs from blood and MLNs, as well as DCs induced from monocytes or $CD34^+$ progenitors in vitro, and explored 1) DC subsets that express a high level of RALDH2, 2) factors that induce human DCs to express a high level of RALDH2, 3) differences between humans and mice in RA-producing DC subsets and RA-inducing factors, 4) intracellular mechanisms by which RALDH2 is induced in DCs, and 5) T cell responses induced by RA-producing DCs in an RA-dependent manner. To quantify the activity of RALDH in mouse (2, 4, 5, 7, 8, 12, 19) and human (5, 19) DCs, recent studies used the Aldefluor reagent that freely diffuses into cells and is converted to a fluorescent product by aldehyde dehydrogenase (ALDH) activity. Thus, we used this reagent in combination with quantitation of ALDH1A2 mRNA to quantify the RA-producing capacity of DCs. We found that only $CD1c^+$ mDCs are capable of expressing a high level of RALDH2 in response to 1α,25-dihydroxyvitamin D_3 (VD_3) together with GM-CSF and that the $RALDH2^{high}$ mDCs induce T cells to preferentially express gut-homing molecules and Th2 cytokines in an RA-dependent manner. This study thus reveals a previously unrecognized distinctive function of human $CD1c^+$ mDCs and an unexpected role of vitamin D, that is, induction of RA from human DCs.

Materials and Methods

Culture media

RPMI 1640 (Nacalai tesque) supplemented with 10% heat-inactivated FCS (ThermoTrace), 2 mM L-glutamine, penicillin G, streptomycin (Life Technologies), and 10 mM HEPES were used for cell culture.

Reagents

Reagents and sources were as follows: recombinant human (rh)TNF, rhIL-3, rh stem cell factor, rhFLT3 ligand (PeproTech); rhGM-CSF (sargramostim; Genzyme); R848 (InvivoGen); LPS (from *Escherichia coli* O111:B4; Sigma-Aldrich); PGE_2 (MP Biomedicals); rhIL-2 (teceleukin; Shionogi & Co.); recombinant mouse GM-CSF (Kirin Brewery); anti-human IL-4 (clone MP4-25D2; eBioscience); anti-human CD28 mAbs (BD Biosciences); LE540 (Wako); U0126 (Cayman Chemical); SB203580, SP600125 (InvivoGen); VX-745 (Tocris); JAK inhibitor I (pyridone 6; Calbiochem); and SB239063 (Enzo Life Sciences). The inhibitors were dissolved in DMSO. Immunomodulatory factors added to DCs are listed in Table I. The following reagents were used for ELISA: anti–human IFN-γ mAb (clone 2G1 as capture Ab), biotinylated anti–human IFN-γ mAb (as detection Ab) and HRP-conjugated streptavidin (Endogen), OptEIA human IL-4 and IL-10 ELISA set (BD Biosciences), human IL-5 ELISA MAX Standard set (BioLegend), and a human IL-13 CytoSets kit (BioSource International).

The following Abs were used to stain human cells and are denoted as "fluorochrome-Ag." FITC-CD45RO, CD14, CD16, CD20, β_7 integrin, and cutaneous lymphocyte Ag (CLA), Alexa Fluor 488-CD1c, PE-CD103, α_4 integrin, and CD203c, PE-Cyanin 5 (PE-Cy5)-CD4, PE-Cyanin 7-CD4, and Brilliant Violet 421-CD11c were from BioLegend; FITC-CD3 and HLA-DR, PE-CD11c and CD25, and PE-Cy5-CD11c from BD Biosciences; allophycocyanin-CD141 from Miltenyi Biotec; allophycocyanin-CCR9 (clone 248621) were from R&D Systems.

The following Abs were used to stain mouse cells and are denoted as fluorochrome-Ag. FITC-B220, PE-CD11c, and allophycocyanin-CD8 were from BD Biosciences; allophycocyanin-CD103 were from BioLegend.

Cell preparations

This study was approved by the Institutional Review Board at Graduate School of Medicine, Kyoto University, and abides by the tenets of the Declaration of Helsinki. All specimens from humans were obtained from healthy donors and patients with written informed consent. To isolate human blood DCs, total PBMCs were depleted of $CD3^+$, $CD14^+$, and $CD16^+$ cells using Dynabeads goat anti-mouse IgG (Invitrogen Dynal). Then, $CD4^+CD11c^+CD141^{-/low}lin^-$ cells ($CD1c^+$ mDCs), $CD4^+CD141^{high}lin^-$ cells ($CD141^{high}$ mDCs), and $CD4^+CD11c^-CD141^{-/low}lin^-$ cells (pDCs) were purified using FACSAria cell sorter (BD Biosciences) (Supplemental Fig. 1A). The expression of CD1c on sorted blood $CD1c^+$ mDCs, $CD141^{high}$ mDCs, and pDCs is shown in Supplemental Fig. 1B. More than 98% of sorted cells were HLA-DR positive (Supplemental Fig. 1C). $CD203c^+$ basophils were isolated by sorting. Naive $CD4^+$ T cells and resting Treg cells (20) were $CD4^{high}CD25^-CD45RO^-$ cells and $CD4^{high}CD25^+CD45RO^-$ cells, respectively. Reanalysis of the sorted cells confirmed a purity of >98%. $CD8^+$ T cells were isolated from PBMCs using CD8 MicroBeads (Miltenyi Biotec).

Human MLNs from patients with colon cancer or Crohn's disease were obtained at Kyoto University Hospital or Hyogo College of Medicine Hospital, respectively. Single-cell suspension of MLNs was obtained by digestion with 500 μg/ml collagenase IV (Wako) and DNase I (Sigma-Aldrich) for 30 min, followed by sorting $CD4^+CD11c^+CD103^+lin^-CD141^{low/int}$ ($CD103^+$ mDCs), $CD4^+CD11c^+CD103^-lin^-CD141^{low/int}$ ($CD103^-$ mDCs), and $CD4^+CD11c^-CD103^-lin^-CD141^{low/int}$ (pDCs) as sorting strategy for blood DCs (Supplemental Fig. 1D). More than 99% of sorted cells were HLA-DR positive (Supplemental Fig. 1E).

Mouse $CD8^+$ and $CD8^-$ splenic DCs were prepared from BALB/c mice as described previously (Supplemental Fig. 1F) (21).

Single-cell suspensions from BALB/c mouse MLNs were prepared by collagenase (Boehringer-Ingerheim) digestion. Low-density cells were separated with BSA gradient centrifugation (Sigma-Aldrich), stained with PE-conjugated anti-CD11c, FITC-conjugated anti-B220, and allophycocyanin-conjugated anti-CD103 mAbs. DCs were first positively enriched using anti-PE microbeads (Mitenyi Biotec), and then, $CD103^+CD11c^+B220^-$ cells and $CD103^-CD11c^+B220^-$ cells were isolated as $CD103^+$ cDCs and $CD103^-$ cDCs, respectively (Supplemental Fig. 1G).

Cell culture

Human blood $CD1c^+$ mDCs, $CD141^{high}$ mDCs, and monocytes were cultured with 800 U/ml GM-CSF for 2 d. Blood pDCs were cultured with 10 ng/ml IL-3 for 2 d. Human mDCs and mouse cDCs from MLNs were cultured with 800 U/ml GM-CSF for 24 h. Human MLN pDCs were cultured with 10 ng/ml IL-3 for 24 h. Mouse splenic cDCs were cultured with 800 U/ml GM-CSF for 24 h. During these cultures, soluble factors (reagents in Table I, TLR ligands, TNF, PGE_2, LE540, or pharmacological inhibitors) were added as indicated. Concentrations of the reagents other than those listed on Table I were 10 μg/ml R848, 1 μg/ml LPS, 100 ng/ml Pam_3CSK_4, 10 ng/ml TNF, 1 μg/ml PGE_2, 1 μM LE540, 20 μM SB203580, 10 μM SP600125, and 20 μM U0126. LE540 and the pharmacological inhibitors were added to the cultures 30 min before adding other reagents. To quantify cell viability, the percentages of propidium iodide–negative cells were measured by flow cytometry after cell debris was excluded by appropriate forward scatter thresholds.

Generation of DCs from monocytes and $CD34^+$ progenitor cells

Monocytes were purified from PBMCs using CD14 MicroBeads (Miltenyi Biotec) and cultured with 800 U/ml GM-CSF and 500 U/ml IL-4 for 7 d to induce immature monocyte-derived DCs (MoDCs). LPS (100 ng/ml) was added during the last 2 d to induce maturation. Immunomodulatory factors (Table I) were added during the whole culture periods. To generate umbilical cord blood $CD34^+$ progenitor cell–derived DCs, $CD34^+$ cells were isolated using CD34 MicroBeads (Miltenyi Biotec) from cord blood and were cultured with 20 ng/ml stem cell factor, 50 ng/ml FLT3 ligand, 800 U/ml GM-CSF, and 2.5 ng/ml TNF for 7 d. Then, the cells were cultured in the absence or presence of RA, VD_3, or LPS (1 μg/ml) for 2 d.

Aldefluor assays and analysis of surface molecules

ALDH activity was determined using the Aldefluor staining kit (StemCell Technology) according to the manufacturer's protocol. Diethylaminobenzaldehyde (DEAB) (Wako) was used as an ALDH inhibitor. T cells cocultured with DCs were stained with mAbs for α_4 integrin, β_7 integrin, CLA, or CCR9. Live cells gated as propidium iodide–negative cells were acquired by FACSCalibur (BD Biosciences). Data were analyzed with FlowJo (Tree Star).

Reverse transcription and real-time PCR

$CD1c^+$ mDCs, $CD141^{high}$ mDCs, and pDCs were cultured with indicated stimuli for 24 h. Total RNA was isolated using Homogenizer and the PureLink RNA Micro Kit (Invitrogen). First-strand cDNA synthesis was performed with the ReverTra Ace qPCR RT Kit (Toyobo). Real-time PCR was performed on the Thermal Cycler Dice Real-Time System (TaKaRa). ALDH1A1, ALDH1A2, ALDH1A3, CYP27B1, vitamin D receptor (VDR), and β-glucronidase (GUSB) were detected using TaqMan Gene Expression Assays (Applied Biosystems) and THUNDERBIRD Probe qPCR Mix (Toyobo). Primer and probe sets were as follows: *ALDH1A1*, Hs00946916_m1; *ALDH1A2*, Hs00180254_m1; *ALDH1A3*, Hs00167476_m1; *CYP27B1*, Hs00168017_m1; *VDR*, Hs01045840_m1; and *GUSB*, Hs00930627_m1.

The mRNA expression levels of each gene were normalized to those of *GUSB*.

T cell cultures with DCs

After extensive wash, $CD1c^+$ mDCs (1×10^4 cells) cultured with GM-CSF, RA, or VD_3 for 2 d were cocultured with allogeneic naive $CD4^+$ T cells or total $CD8^+$ T cells (1×10^5 cells) in the absence or presence of 1 μM LE540, 10 μg/ml rat IgG1, or 10 μg/ml anti–IL-4 mAb in 96-well U-bottom plates for 6 d. IL-2 (10 U/ml) was added to $CD8^+$ T cell culture. The $CD4^+$ T cells were restimulated at 1×10^6 cells/ml with plate-bound anti-CD3 (OKT3) and 1 μg/ml soluble anti-CD28 mAbs in 96-well flat-bottom plates for 24 h. The supernatants were analyzed for cytokines by ELISA.

Statistical analysis

Data are presented as the mean ± SE. Statistical comparisons were performed using paired two-tailed *t* test. Difference with $p < 0.05$ was considered significant.

Results

Human blood $CD1c^+$ mDCs, but not $CD141^{high}$ mDCs, express a high level of RALDH2 in response to GM-CSF and VD_3

In search of human DCs that express a high level of RALDH enzymes, different subsets of blood DCs were treated with various factors that have been reported to modulate immunostimulatory activity of DCs (Table I), and ALDH activity was measured with Aldefluor (2, 4, 5, 7, 8, 12, 19). To keep mDCs alive, we added GM-CSF (22) to $CD1c^+$ mDCs. GM-CSF by itself induced little ALDH activity (Fig. 1A, 1B). Adding RA with GM-CSF only slightly induced the activity, whereas VD_3, which modulates immunostimulatory properties of human mDCs and MoDCs (23–25), together with GM-CSF strongly upregulated the ALDH activity in $CD1c^+$ mDCs. RA plus VD_3 further augmented it (Fig. 1A, 1B). RA and VD_3 without GM-CSF induced little ALDH activity (Fig. 1A), indicating that GM-CSF is necessary for the induction. Ligands for TLRs (R848, LPS, and Pam_3CSK_4) and TNF strongly suppressed the ALDH activity, but PGE_2, which has been reported to suppress the ALDH activity in mouse bone marrow DCs (19), did not (Fig. 1C). There were no substantial differences in cell viability between different culture conditions at the time of harvest (data not shown). None of the other immunomodulatory factors (Table I) upregulated the ALDH activity in combination with GM-CSF (Supplemental Fig. 2).

In contrast to $CD1c^+$ mDCs, $CD141^{high}$ mDCs (Fig. 1D), pDCs (Fig. 1E), and CD34-derived DCs (Fig. 1F) cultured with RA and VD_3 exhibited little ALDH activity. RA and VD_3 without or with LPS slightly induced ALDH activity in MoDCs but at far lower levels than that in $CD1c^+$ mDCs (Fig. 1G). Consistent with a previous observation that human basophils express RALDH2 in response to IL-3 (26), IL-3 alone induced ALDH activity in basophils, but there was no augmentation with RA and VD_3 (Fig. 1H). There were no substantial differences in cell viability between different culture conditions (data not shown). Again, none of the other factors (Table I) upregulated the ALDH activity in combination with GM-CSF ($CD141^{high}$ mDCs, MoDCs) or IL-3 (pDCs) (Supplemental Fig. 2).

Table I. Immunomodulatory factors added to DCs

Name	Concentrations	Sources
RA	10 nM	Wako
VD_3	10 nM	Wako
IFN-α	1000 U/ml	Intron A, Schering-Plough
IL-4	500 U/ml	PeproTech
TGF-β	10 ng/ml	PeproTech
Vasoactive intestinal peptide	100 nM	LKT Laboratories
Rosiglitazone	10 μM	Alexis Biochemicals
T0901317	1 μM	Cayman Chemicals
Rapamycin	100 ng/ml	PeproTech
Tacrolimus	100 ng/ml	Enzo Life Sciences
Cyclosporin A	1000 ng/ml	Sigma-Aldrich
Dexamethasone	1 μM	Sigma-Aldrich

We also cultured monocytes with GM-CSF in the absence or presence of the immunomodulatory factors (Table I). RA plus VD_3 substantially induced ALDH activity, albeit to a lesser extent than that in $CD1c^+$ mDCs. None of the other factors substantially induced the activity (Supplemental Fig. 2).

We next examined whether the ALDH activity detected by Aldefluor correlates with the expression levels of mRNA for *ALDH1A2* (encoding RALDH2) in $CD1c^+$ mDCs, $CD141^{high}$ mDCs, and pDCs. Consistent with the results by Aldefluor analyses, GM-CSF alone induced little expression of ALDH1A2 mRNA in $CD1c^+$ mDCs, and the addition of VD_3 markedly upregulated it (Fig. 1I). The addition of RA to GM-CSF and to GM-CSF plus VD_3 slightly increased the expression of ALDH1A2 mRNA, but R848 completely suppressed it. There was almost no expression of ALDH1A2 mRNA in $CD141^{high}$ mDCs or pDCs. mRNAs for *ALDH1A1* and *ALDH1A3* (encoding RALDH1 and RALDH3) were hardly expressed in $CD1c^+$ mDCs even in the presence of the indicated stimulation (Fig. 1J, 1K).

Collectively, 1) $CD1c^+$ mDCs, but not the other human blood DC subsets, express a high level of RALDH2 in response to GM-CSF plus VD_3, and exogenous RA augments the expression, and 2) proinflammatory factors (TLR ligands and TNF) suppress the expression of RALDH2.

Human $CD103^-$ mDCs in MLNs gain ALDH activity in response to the VD_3-containing stimulus

To examine whether human MLN DCs exhibit ALDH activity as mouse MLN $CD103^+$ DCs do (3, 4), DC subsets were isolated from MLNs of patients with colon cancer or Crohn's disease in the same way as done for blood DCs (Supplemental Fig. 1D). Unlike in blood, $CD141^{high}$ mDCs were not identified as a discrete population in MLNs. $CD11c^{high}$ mDCs were subdivided into $CD103^+$ and $CD103^-$ mDCs. pDCs did not express CD103.

Unlike mouse MLN DCs, freshly isolated human $CD103^+$ MLN mDCs did not have ALDH activity (Fig. 2). Unexpectedly, $CD103^-$ but not $CD103^+$ MLN mDCs gained a high level of ALDH activity in response to GM-CSF, RA, and VD_3. pDCs did not exhibit ALDH activity. All the above results were the same in DCs from both colon cancer and Crohn's disease. Thus, in humans, $CD103^-$ but not $CD103^+$ MLN mDCs may be RA-producing DCs in situ in the intestine.

Mouse splenic and MLN cDCs gain ALDH activity in response to GM-CSF alone

Genome-wide expression profiling clustered human $CD141^{high}$ mDCs and $CD1c^+$ mDCs with mouse $CD8^+$ cDCs and $CD8^-$ cDCs, respectively (18). Thus, we examined whether VD_3 differentially induces mouse splenic cDC subsets to gain ALDH activity. As we reported (4), GM-CSF alone was sufficient to induce high levels of ALDH activity in both $CD8^+$ DCs and $CD8^-$ DCs in the spleen (Fig. 3A). Neither RA nor VD_3 augmented the activity. Unlike in human $CD1c^+$ mDCs, LPS did not suppress it. There were no substantial differences in cell viability between different culture conditions (data not shown). We also examined ALDH activity in mouse MLN cDCs in the absence or presence of the VD_3-containing stimulus. As reported (3), fresh $CD103^+$ but not $CD103^-$ cDCs in MLNs exhibited ALDH activity (Fig. 3B). Again, GM-CSF alone was sufficient to induce high levels of ALDH activity in both $CD103^+$ and $CD103^-$ cDCs, and the addition of RA and VD_3 did not augment it.

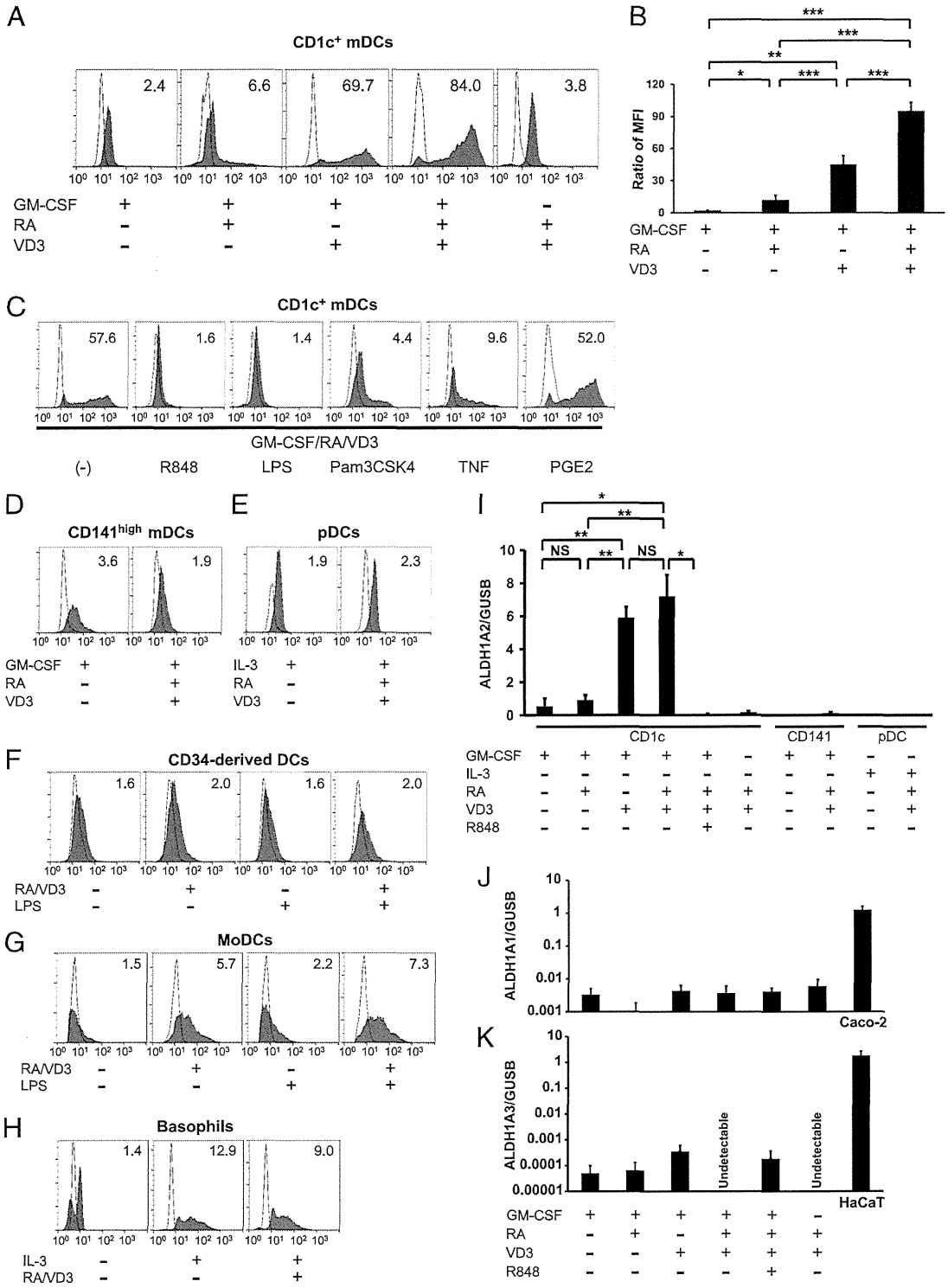

FIGURE 1. ALDH activity and ALDH1A2 mRNA expression in human blood DC subsets and basophils. CD1c$^+$ mDCs (**A–C**), CD141^{high} mDCs (**D**), pDCs (**E**), and basophils (**H**) were cultured in the absence or presence of the indicated reagents for 2 d. CD34$^+$ progenitor cell–derived dendritic cells (CD34-derived DCs) (**F**) and MoDCs (**G**) were cultured as indicated in *Materials and Methods*. The cells were incubated with Aldefluor in the absence (solid histograms) or presence (open histograms) of an ALDH inhibitor DEAB and were analyzed by flow cytometry. The numbers shown with each histogram represent ratios of mean fluorescence intensity of Aldefluor in the absence of DEAB to that in the presence of DEAB. (**I**) ALDH1A2 mRNA expression was measured by real-time RT-PCR. CD1c$^+$ mDCs, CD141^{high} mDCs, and pDCs were cultured with the indicated stimuli for 24 h. The expression levels were normalized to those of GUSB. $*p < 0.05$, $**p < 0.01$, $***p < 0.001$. ALDH1A1 (**J**) and ALDH1A3 (**K**) mRNA expressions were measured by real-time RT-PCR. CD1c$^+$ mDCs were cultured with the indicated stimuli for 24 h. Human colon cancer cell line Caco-2 and human keratinocyte cell line HaCaT were used as positive controls for ALDH1A1 and ALDH1A3, respectively. The expression levels were normalized to those of GUSB. Note the low levels of the scales. The data are representative of three (A, D–G) or two (H) independent experiments and are shown as the mean ± SE of 8 (B), 4 (I), or 3 (J, K) independent experiments.

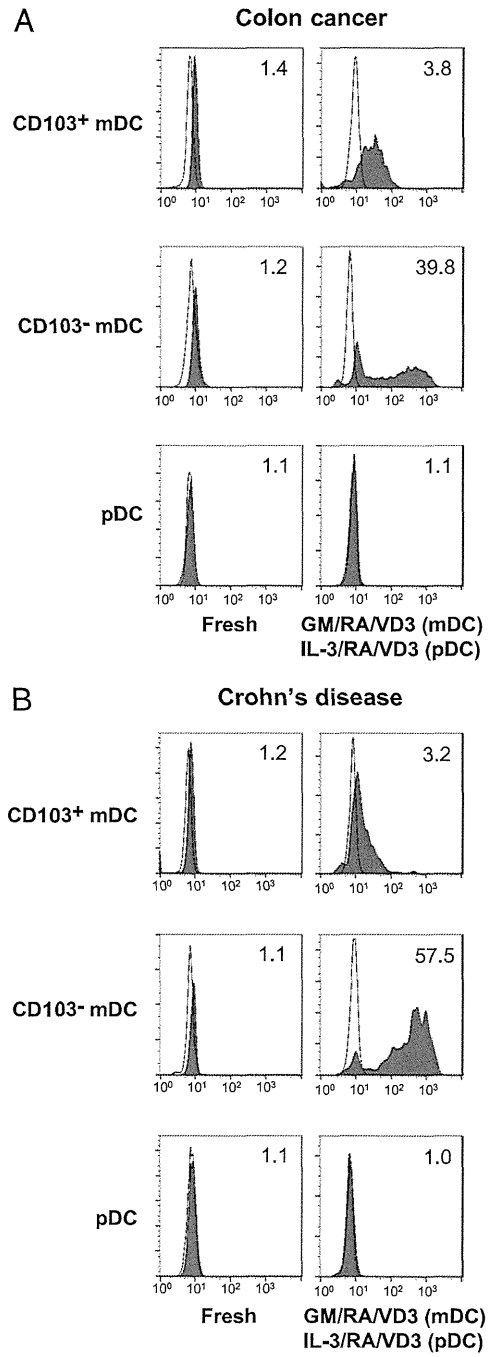

FIGURE 2. ALDH activity in human MLN DC subsets. $CD103^+$ mDCs, $CD103^-$ mDCs, or pDCs were purified from MLNs of patients with colon cancer (**A**) or Crohn's disease (**B**) and were analyzed without culture or after culture with the indicated stimuli for 24 h. Histograms and the numbers shown with them are presented as in Fig. 1. The data are representative of three (A) or two (B) independent experiments.

Collectively, the RA-producing DC subsets and the stimulation to induce RA production are different between human and mouse DCs, in that 1) both of the cDC subsets in mouse spleen ($CD8^+$ and $CD8^-$) and MLNs ($CD103^+$ and $CD103^-$) exhibit ALDH activity in response to GM-CSF alone, 2) VD_3 does not induce or increase the activity, and 3) TLR signaling does not suppress the activity in mice.

Engagement of RA receptor is necessary for the high level of RALDH2 expression induced by VD_3

We investigated the mechanisms by which GM-CSF, RA, and VD_3 induce a high level of RALDH2 in human $CD1c^+$ mDCs. Exogenous RA augmented the expression of RALDH2 induced by VD_3 (Fig. 1A, 1B). Thus, we examined whether endogenous RA is responsible for the induction of RALDH2 by VD_3. A pan-RA receptor (RAR) antagonist LE540 diminished the induction of ALDH activity by VD_3 (Fig. 4A), indicating that endogenous RA or possibly RAR agonists contained in the serum are necessary for the induction of a high level of RALDH2 by VD_3. However, the induction of RALDH2 by RA alone was much weaker than the induction by VD_3 (Fig. 1A, 1B), indicating that combined signals by RA and VD_3 are necessary for the full expression of RALDH2.

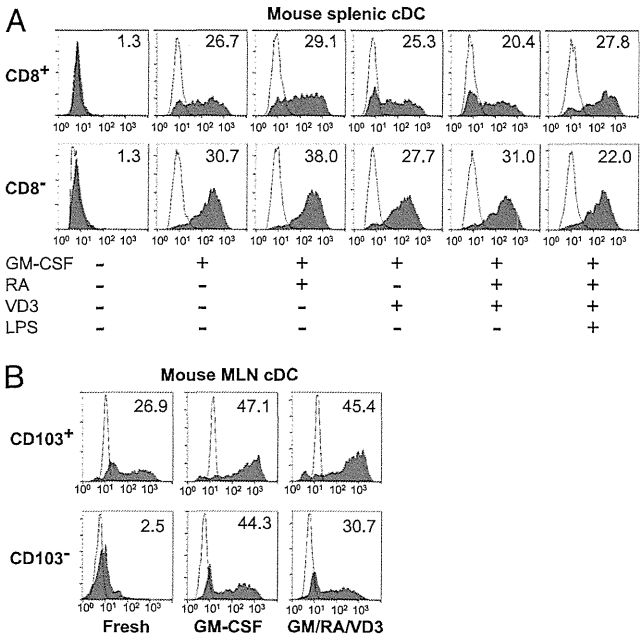

FIGURE 3. ALDH activity in mouse splenic and MLN cDC subsets. (**A**) $CD8^+$ and $CD8^-$ mouse splenic cDCs were cultured without or with the indicated stimuli for 24 h. (**B**) $CD103^+$ and $CD103^-$ mouse MLN cDCs were analyzed without culture or were cultured with the indicated stimuli for 24 h. Histograms and the numbers shown with them are presented as in Fig. 1. The data are representative of three independent experiments.

When cultured with GM-CSF, RA, and VD_3, $CD1c^+$ mDCs expressed only a low level of mRNA for CYP27B1, the enzyme that converts 25-hydroxyvitamin D_3 into its bioactive form VD_3 (27), although $CD1c^+$ mDCs expressed a high level of CYP27B1 mRNA in the presence of R848 (Supplemental Fig. 3A). Thus, endogenous VD_3 does not appear to participate in the induction of RALDH2.

$CD1c^+$ mDCs, $CD141^{high}$ mDCs, and pDCs expressed similar levels of mRNA for the nuclear VDR, consistent with a previous report (Supplemental Fig. 3B) (25). Thus, the marked effect of VD_3 on the induction of RALDH2 in $CD1c^+$ mDCs is not likely to be determined by differential expression of VDR among the DC subsets, but $CD1c^+$ mDCs may have distinctive molecular machineries to express RALDH2 in response to VD_3.

Activation of p38 is necessary for the induction of RALDH2

We investigated signaling pathways involved in the induction of RALDH2 in $CD1c^+$ mDCs. After stimulation with GM-CSF, RA, and VD_3, the DCs started to express ALDH1A2 mRNA at 6 h, and the expression reached its peak at 24 h (Fig. 4B). This slow kinetics indicates that the induction of ALDH1A2 mRNA is not due to direct transcriptional activity of VDR. Instead, secondary signals downstream of VDR and RAR are likely to mediate the induction of ALDH1A2 mRNA.

A pan-JAK inhibitor strongly blocked the induction of ALDH activity (Fig. 4C) in accord with the dependence of the induction

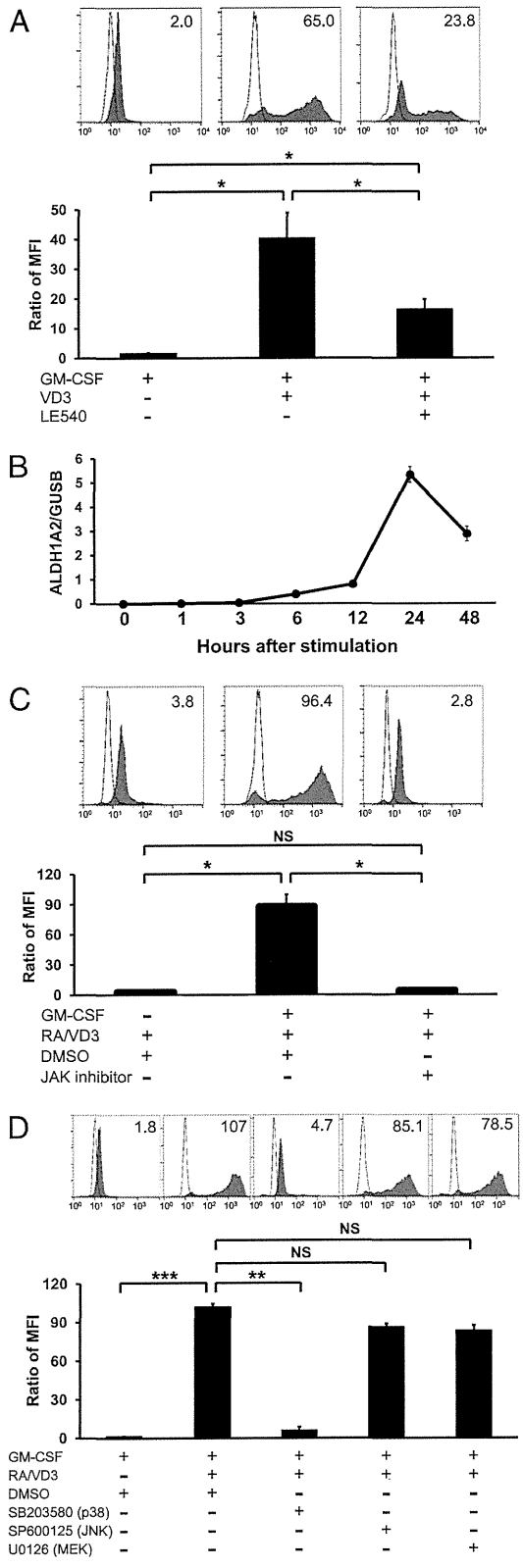

FIGURE 4. The induction of ALDH activity in CD1c$^+$ mDCs is dependent on RAR, JAK, and p38 signaling. (**A**, **C**, and **D**) CD1c$^+$ mDCs were cultured with the indicated reagents for 2 d. Histograms and the numbers shown with them are presented as in Fig. 1. The histograms are representative data, and the graphs show the mean ± SE of four (A) or three (C, D) independent experiments. (**B**) CD1c$^+$ mDCs were cultured with GM-CSF, RA, and VD_3 for the indicated time periods. ALDH1A2 mRNA expressions were measured by real-time RT-PCR. The expression levels were normalized to those of GUSB. The data are presented as the mean ± SD of duplicate samples in one of two independent experiments.

on GM-CSF. Three p38 MAPK inhibitors, SB203580 (Fig. 4D), SB239063 (28), and VX-745 (29) (data not shown), also blocked the induction. In contrast, inhibitors against JNK (SP600125) or MEK 1/2 (U0126) did not do so (Fig. 4D). There were no substantial differences in cell viability between different culture conditions (data not shown). Thus, RALDH2 in CD1c$^+$ mDCs is induced in a p38-dependent manner.

RALDH2^{high} mDCs induce T cells to acquire gut-homing capacities in an RA-dependent manner

RA derived from mouse intestinal DCs endows T cells with the expression of gut-homing molecules, $\alpha_4\beta_7$ integrin and CCR9 (1). Furthermore, intestinal DCs reciprocally suppress the expression of skin-homing molecules, P- and L-selectin ligands, on T cells (30). Thus, we examined homing properties of T cells stimulated with GM-CSF/RA/VD_3–treated RALDH2^{high}CD1c$^+$ mDCs (hereafter referred to as RALDH2^{high} mDCs). Naive CD4$^+$ T cells stimulated with allogeneic RALDH2^{high} mDCs expressed a higher level of $\alpha_4\beta_7$ integrin (Fig. 5A, 5B) and reciprocally a lower level of a P- and L-selectin ligand CLA (Fig. 5C) than T cells stimulated with GM-CSF–treated RALDH2^{low}CD1c$^+$ mDCs (hereafter referred to as RALDH2^{low} mDCs). The upregulation of $\alpha_4\beta_7$ integrin and downregulation of CLA by RALDH2^{high} mDCs were abrogated by LE540. These data indicate that RALDH2^{high} mDCs induce gut-homing and reduce skin-homing properties of T cells in an RA-dependent manner. RALDH2^{high} mDCs did not induce allogeneic naive CD4$^+$ T cells or total CD8$^+$ T cells to express a detectable level of CCR9 (data not shown).

RALDH2^{high} mDCs induce naive CD4$^+$ T cells to acquire Th2 cytokine–producing capacities in an RA-dependent manner

We examined cytokine-producing properties of naive CD4$^+$ T cells stimulated with allogeneic mDCs. CD4$^+$ T cells stimulated with RALDH2^{high} mDCs secreted significantly higher levels of Th2 cytokines IL-4, IL-5, and IL-13 than those stimulated with RALDH2^{low} mDCs (Fig. 6A). This effect was abrogated by LE540 (Fig. 6A), but not by anti–IL-4 neutralizing mAb (Fig. 6B). CD4$^+$ T cells stimulated with RALDH2^{high} mDCs secreted a similar level of IFN-γ, compared with those stimulated with RALDH2^{low} mDCs (Fig. 6C). CD4$^+$ T cells stimulated with RALDH2^{high} mDCs secreted a significantly higher level of IL-10 than those stimulated with RALDH2^{low} mDCs, but the induction of IL-10 was not abrogated by LE540 (Fig. 6C). These data indicate that RALDH2^{high} mDCs induce naive CD4$^+$ T cells to acquire the ability to produce high levels of Th2 cytokines in an RA-dependent and IL-4–independent manner.

We also examined whether naive CD4$^+$ T cells stimulated with RALDH2^{high} mDCs acquire regulatory activity. Although CD4$^+$ T cells stimulated with RALDH2^{high} mDCs slightly suppressed proliferation of concomitant T cells, the effect was much weaker than that exhibited by resting Treg cells directly purified from blood (20) (data not shown). Thus, RALDH2^{high} mDCs do not have an unambiguous regulatory T cell–inducing ability detectable by our assay.

Discussion

RA plays a critical role in maintaining immune homeostasis in the intestine (27). Human DCs that produce a high level of RA remained unknown. The present study identifies blood CD1c$^+$ mDCs as a DC subset that potently produces RA in response to VD_3 in humans. RALDH2^{high} CD1c$^+$ mDCs induced T cells to preferentially express gut-homing molecules and Th2 cytokines in an RA-dependent manner. This study reveals a novel component in

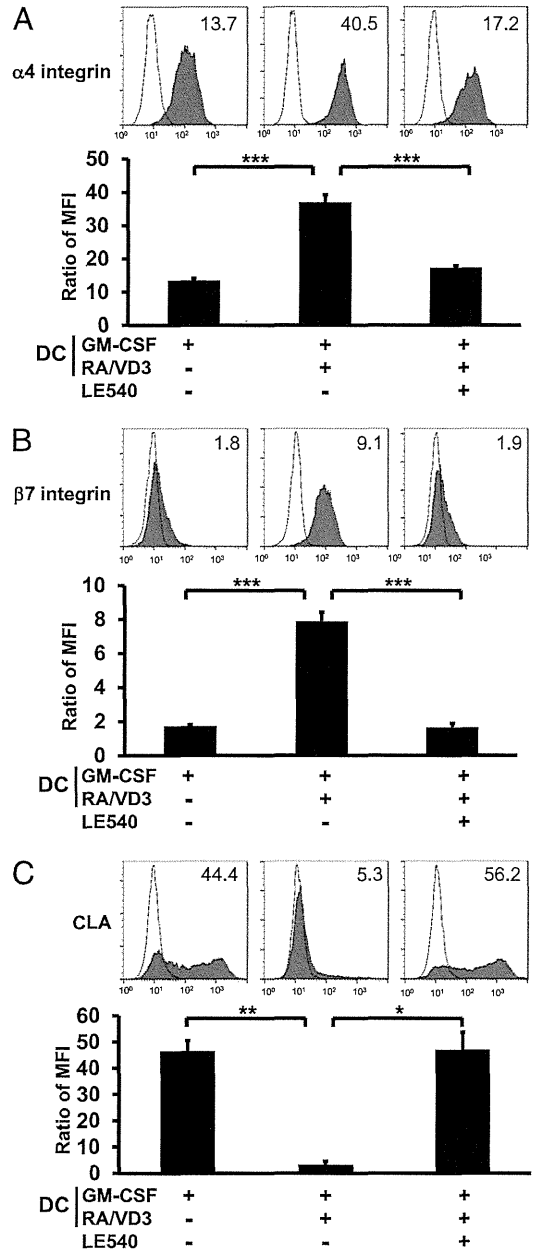

FIGURE 5. RALDH2^{high} mDCs induce gut-homing and suppress skin-homing molecules on CD4$^+$ T cells in an RA-dependent manner. CD1c$^+$ mDCs were cultured with GM-CSF alone (RALDH2^{low} mDCs) or GM-CSF, RA, and VD_3 (RALDH2^{high} mDCs) for 2 d. The DCs were collected and extensively washed. Then allogeneic naive CD4$^+$ T cells were stimulated with RALDH2^{low} mDCs or RALDH2^{high} mDCs in the absence or presence of LE540 for 6 d. The T cells were stained for α_4 integrin (**A**), β_7 integrin (**B**), or CLA (**C**). Open histograms represent cells stained with isotype-matched control mAbs. The numbers shown with each histogram represent ratios of mean fluorescence intensity (MFI) of each surface molecule to that of isotype-matched control. The histograms are representative data, and the graphs show the mean ± SE from six (A, B) or three (C) independent experiments. $*p < 0.05$, $**p < 0.01$, $***p < 0.001$.

the immune system in humans, that is, a "vitamin D – CD1c$^+$ mDC – RA" axis for immune regulation.

Which DCs produce RA will be determined by two factors: 1) environmental signals DCs receive, and 2) intrinsic nature of each DC subset. In mice, RA (4–8), GM-CSF (4), IL-4 (4, 9), and TLR ligands (2, 4, 5, 10–12) induce DCs to express RALDH2. In humans, RA (5), Pam_3CSK_4 (5, 12), and a peroxisome proliferator–activated receptor γ ligand (rosiglitazone) (31) augment the expression of RALDH2 in MoDCs. In this study, to our knowledge, we demonstrated for the first time that VD_3 induces CD1c$^+$ mDCs to express a high level of RALDH2 in the presence of GM-CSF. Whereas exogenous RA moderately augmented the induction, neither IL-4 nor various immunomodulatory reagents including rosiglitazone augmented it. Notably, proinflammatory factors, TLR ligands and TNF, strongly suppressed ALDH activity. These data suggest that VD_3 is a key factor to induce human CD1c$^+$ mDCs to express RALDH2 in the steady state.

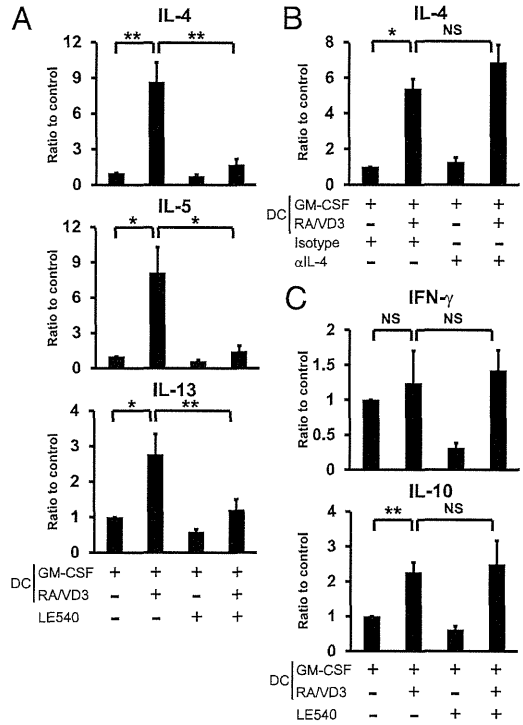

FIGURE 6. RALDH2^{high} mDCs induce CD4$^+$ T cells to produce Th2 cytokines in an RA-dependent manner. CD1c$^+$ mDCs were cultured as in Fig. 5 and were collected and extensively washed. Then allogeneic naive CD4$^+$ T cells were cocultured with RALDH2^{low} mDCs or RALDH2^{high} mDCs in the absence or presence of LE540 for 6 d (**A**, **C**) or in the presence of rat IgG1 (isotype) or anti–IL-4 mAb (**B**). The stimulated T cells were restimulated for 24 h, and the supernatants were analyzed for cytokines by ELISA. The data are normalized to the value obtained from CD4$^+$ T cells cocultured with RALDH2^{low} mDCs in the absence of LE540 or anti–IL-4 mAb. The data are shown as the mean ± SE of eight (A, C) or three (B) independent experiments. $*p < 0.05$, $**p < 0.01$. The mean and ranges of absolute cytokine concentrations from T cells cocultured with RALDH2^{low} mDCs in the absence of LE540 or anti–IL-4 mAb were as follows: (A) IL-4, 79.5 pg/ml (46.8–145 pg/ml); IL-5, 57.9 pg/ml (15.6–122 pg/ml); IL-13, 1720 pg/ml (321–4547 pg/ml); (B) IL-4, 63.9 pg/ml (42.9–104 pg/ml); and (C) IFN-γ, 28.5 ng/ml (9.48–80.6 ng/ml), and IL-10, 219 pg/ml (93.6–416 pg/ml).

It has been shown that VD_3 inhibits the expression of RALDH2 in mouse DCs (32). In addition, VD_3 represses RA-transcriptional activity via VDR in human myeloid cells (33). These findings indicate that VD_3 antagonizes the activity of RA. Thus, the cooperation between exogenous VD_3 and endogenously induced RA for the induction of RALDH2 in human CD1c$^+$ mDCs was unexpected. These results indicate that signaling pathways triggered by RA and VD_3 may antagonize or synergize, depending on cell types, coexisting factors, and/or species.

Among the human DC subsets we examined, CD1c$^+$ mDCs was the only subset that expresses a high level of RALDH2 in response to VD_3. Human CD141^{high} mDCs and their equivalent, mouse CD8$^+$CD11b$^-$ cDCs in lymphoid tissues (18) and CD103$^+$ cDC in

nonlymphoid tissues (17), share capacities to efficiently cross-present Ags to $CD8^+$ T cells (14–17). In contrast, distinctive functions of $CD1c^+$ mDCs, an equivalent of mouse $CD8^-CD11b^+$ cDCs (18), have been elusive. The present study suggests that, in contrast to $CD141^{high}$ mDCs, $CD1c^+$ mDCs may function as immunoregulatory DCs by preferentially producing RA upon exposure to VD_3.

Although several studies have shown that human MoDCs express RALDH2 (5, 12, 19, 31), gene expression profiling has shown that MoDCs markedly differ from the three subsets of human DCs in blood and lymphoid tissues and are more similar to macrophages (18). In addition, it remains to be determined to what extent monocytes differentiate into DCs in vivo in humans. Thus, the RALDH2 expression in $CD1c^+$ mDCs is likely to be more relevant to DC biology in vivo than that in MoDCs. Intriguingly, monocytes but not MoDCs exhibited a substantial level of ALDH activity in response to GM-CSF, RA, and VD_3, suggesting that $CD1c^+$ mDCs and monocytes may have similar machinery to express RALDH2.

Whereas freshly isolated mouse intestinal $CD103^+$ DCs but not $CD103^-$ DCs produce RA (3), we showed that 1) freshly isolated human MLN DCs do not have ALDH activity and that 2) $CD103^-$ mDCs but not $CD103^+$ mDCs in MLNs gain a high level of ALDH activity in response to the VD_3-containing stimulus. Although our data does not clarify the relationship between mouse and human DC subsets in MLNs, the data suggest that CD103 may not be a marker of DCs that preferentially produce RA in human MLNs. Jaesson et al. (34) reported that $CD103^+$ DCs from human MLNs induce T cells to express $\alpha_4\beta_7$ integrin and CCR9 in an RAR signaling–dependent manner. However, such DCs neither exhibited ALDH activity (Fig. 2A, 2B) nor induced T cells to express these gut-homing molecules (data not shown) in our experiments. Because Jaesson et al. (34) did not directly examine ALDH activity of MLN DCs, the reason for the discrepancy between the two studies is not clear.

Furthermore, GM-CSF alone was sufficient to induce high levels of ALDH activity in both of the cDC subsets in mouse spleen ($CD8^+$ and $CD8^-$) and MLNs ($CD103^+$ and $CD103^-$), and VD_3 did not augment the activity. Thus, DC subsets capable of acquiring ALDH activity and the stimulation to induce DCs to acquire the activity appear to be significantly different between humans and mice.

RA (5) or zymosan (11) induces mouse splenic DCs to express RALDH2 through RAR or TLR2, respectively, in an ERK-dependent manner. Pam_3CSK_4 induces mouse splenic DCs to express RALDH2 in a JNK-dependent manner (12). In contrast, we showed that p38 but not MEK or JNK is necessary to induce human $CD1c^+$ mDCs to express RALDH2 in response to VD_3. Thus, although MAPK is important for the induction of RALDH2 in DCs, it appears that which MAPK is involved depends on the type of stimuli and/or species.

Although $RALDH2^{high}$ $CD1c^+$ mDCs induced the expression of a higher level of $\alpha_4\beta_7$ integrin and reciprocally suppressed the expression of CLA on T cells in an RA-dependent manner, we could not observe the induction of CCR9 in the culture conditions we used. Spiegl et al. (26) also reported no CCR9 induction on human T cells by RA. Thus, the induction of CCR9 on human T cells may be more tightly regulated than that on mouse T cells.

VD_3 directly acts on T cells to induce skin-homing receptors (35). The present study showed that VD_3 induces T cells to express gut-homing receptors through inducing RA production by DCs. It appears to be difficult to reconcile these two phenomena. A possible scenario is that $CD1c^+$ mDCs are exposed to VD_3 in peripheral tissues, migrate into regional lymph nodes, and present RA to T cells. Indeed, tissue-resident cells such as epithelial cells and macrophages (36) express CYP27B1. As such, exposure of DCs to VD_3 may be spatially and chronologically separated from T cell stimulation by the DCs.

VD_3 and RA have been thought to reciprocally control immune responses in the skin and intestine (27). Thus, the induction of RALDH2 by VD_3 is counterintuitive. However, such dichotomy between VD_3 and RA are becoming blurred. On the one hand, VD_3 locally produced by epithelial cells and macrophages in various organs and lymphoid tissues (36) likely has an immunomodulatory effect in a paracrine manner (37). On the other hand, RA-producing DCs exist in extraintestinal as well as intestinal tissues and their corresponding draining lymph nodes (2). In addition, a wide variety of cells can produce GM-CSF. Thus, VD_3, RA, and GM-CSF are likely to have opportunities to collaborate and to stimulate $CD1c^+$ mDCs in various tissues, and such DCs may induce gut-homing T cells by producing RA in extraintestinal as well as intestinal compartments.

$RALDH2^{high}$ mDCs induced naive $CD4^+$ T cells to acquire the ability to produce Th2 cytokines in an RA-dependent and IL-4–independent manner. The apparently direct effect of RA on Th2 induction is consistent with our previous report with mice (38). It has been shown that RA derived from basophils also induces Th2 cells (26). Thus, RA derived from $CD1c^+$ mDCs as well as basophils may contribute to Th2 polarization.

It has been proposed that Th2-type allergic responses may constitute an important asset of the immune system to maintain tissue homeostasis by ameliorating inflammation and promoting tissue repair (39, 40). The present study suggests that locally produced VD_3 may induce RA-producing $CD1c^+$ mDCs that promote a "type 2" environment, thus contributing to maintaining tissue homeostasis. Inflammation caused by infections, exemplified by the stimulation of $CD1c^+$ mDCs with TLR ligands and TNF, may extinguish the Th2-inducing RA production, and turn on type 1 inflammation. Taken together with a recent report that VD_3-stimulated $CD1c^+$ blood mDCs produce IL-10 and induce Treg cells (41), $CD1c^+$ mDCs may represent a DC subset that maintains immune homeostasis. Furthermore, epidemiological studies have shown that a poor vitamin D status is associated with an increased risk of autoimmune diseases (37). Thus, it is intriguing to speculate that RA production by $CD1c^+$ mDCs stimulated with VD_3 contributes to prevention of autoimmune diseases in the steady state.

In conclusion, this study reveals a novel link between two key immunomodulatory vitamins (vitamin A and D) via a distinctive human DC subset, that is, $CD1c^+$ mDCs. This may constitute a previously unrecognized immune component for maintaining tissue homeostasis. Exploiting immunomodulatory activity of this component may lead to novel therapies or prevention of various autoimmune or inflammatory disorders.

Acknowledgments

We thank Keiko Fukunaga for excellent technical assistance.

Disclosures

The authors have no financial conflicts of interest.

References

1. Iwata, M., A. Hirakiyama, Y. Eshima, H. Kagechika, C. Kato, and S.-Y. Song. 2004. Retinoic acid imprints gut-homing specificity on T cells. *Immunity* 21: 527–538.
2. Guilliams, M., K. Crozat, S. Henri, S. Tamoutounour, P. Grenot, E. Devilard, B. de Bovis, L. Alexopoulou, M. Dalod, and B. Malissen. 2010. Skin-draining lymph nodes contain dermis-derived $CD103^-$ dendritic cells that constitutively produce retinoic acid and induce $Foxp3^+$ regulatory T cells. *Blood* 115: 1958–1968.
3. Coombes, J. L., K. R. R. Siddiqui, C. V. Arancibia-Cárcamo, J. Hall, C.-M. Sun, Y. Belkaid, and F. Powrie. 2007. A functionally specialized population of mu-

cosal CD103$^+$ DCs induces Foxp3$^+$ regulatory T cells via a TGF-β and retinoic acid-dependent mechanism. *J. Exp. Med.* 204: 1757–1764.
4. Yokota, A., H. Takeuchi, N. Maeda, Y. Ohoka, C. Kato, S.-Y. Song, and M. Iwata. 2009. GM-CSF and IL-4 synergistically trigger dendritic cells to acquire retinoic acid-producing capacity. *Int. Immunol.* 21: 361–377.
5. Villablanca, E. J., S. Wang, J. de Calisto, D. C. O. Gomes, M. A. Kane, J. L. Napoli, W. S. Blaner, H. Kagechika, R. Blomhoff, M. Rosemblatt, et al. 2011. MyD88 and retinoic acid signaling pathways interact to modulate gastrointestinal activities of dendritic cells. *Gastroenterology* 141: 176–185.
6. Feng, T., Y. Cong, H. Qin, E. N. Benveniste, and C. O. Elson. 2010. Generation of mucosal dendritic cells from bone marrow reveals a critical role of retinoic acid. *J. Immunol.* 185: 5915–5925.
7. Molenaar, R., M. Knippenberg, G. Goverse, B. J. Olivier, A. F. de Vos, T. O'Toole, and R. E. Mebius. 2011. Expression of retinaldehyde dehydrogenase enzymes in mucosal dendritic cells and gut-draining lymph node stromal cells is controlled by dietary vitamin A. *J. Immunol.* 186: 1934–1942.
8. Jaensson-Gyllenbäck, E., K. Kotarsky, F. Zapata, E. K. Persson, T. E. Gundersen, R. Blomhoff, and W. W. Agace. 2011. Bile retinoids imprint intestinal CD103$^+$ dendritic cells with the ability to generate gut-tropic T cells. *Mucosal Immunol.* 4: 438–447.
9. Elgueta, R., F. E. Sepulveda, F. Vilches, L. Vargas, J. R. Mora, M. R. Bono, and M. Rosemblatt. 2008. Imprinting of CCR9 on CD4 T cells requires IL-4 signaling on mesenteric lymph node dendritic cells. *J. Immunol.* 180: 6501–6507.
10. Uematsu, S., K. Fujimoto, M. H. Jang, B.-G. Yang, Y.-J. Jung, M. Nishiyama, S. Sato, T. Tsujimura, M. Yamamoto, Y. Yokota, et al. 2008. Regulation of humoral and cellular gut immunity by lamina propria dendritic cells expressing Toll-like receptor 5. *Nat. Immunol.* 9: 769–776.
11. Manicassamy, S., R. Ravindran, J. Deng, H. Oluoch, T. L. Denning, S. P. Kasturi, K. M. Rosenthal, B. D. Evavold, and B. Pulendran. 2009. Toll-like receptor 2-dependent induction of vitamin A-metabolizing enzymes in dendritic cells promotes T regulatory responses and inhibits autoimmunity. *Nat. Med.* 15: 401–409.
12. Wang, S., E. J. Villablanca, J. De Calisto, D. C. O. Gomes, D. D. Nguyen, E. Mizoguchi, J. C. Kagan, H.-C. Reinecker, N. Hacohen, C. Nagler, et al. 2011. MyD88-dependent TLR1/2 signals educate dendritic cells with gut-specific imprinting properties. *J. Immunol.* 187: 141–150.
13. Ziegler-Heitbrock, L., P. Ancuta, S. Crowe, M. Dalod, V. Grau, D. N. Hart, P. J. M. Leenen, Y.-J. Liu, G. MacPherson, G. J. Randolph, et al. 2010. Nomenclature of monocytes and dendritic cells in blood. *Blood* 116: e74–e80.
14. Jongbloed, S. L., A. J. Kassianos, K. J. McDonald, G. J. Clark, X. Ju, C. E. Angel, C.-J. J. Chen, P. R. Dunbar, R. B. Wadley, V. Jeet, et al. 2010. Human CD141$^+$ (BDCA-3)$^+$ dendritic cells (DCs) represent a unique myeloid DC subset that cross-presents necrotic cell antigens. *J. Exp. Med.* 207: 1247–1260.
15. Poulin, L. F., M. Salio, E. Griessinger, F. Anjos-Afonso, L. Craciun, J.-L. Chen, A. M. Keller, O. Joffre, S. Zelenay, E. Nye, et al. 2010. Characterization of human DNGR-1$^+$BDCA3$^+$ leukocytes as putative equivalents of mouse CD8α+ dendritic cells. *J. Exp. Med.* 207: 1261–1271.
16. Bachem, A., S. Güttler, E. Hartung, F. Ebstein, M. Schaefer, A. Tannert, A. Salama, K. Movassaghi, C. Opitz, H. W. Mages, et al. 2010. Superior antigen cross-presentation and XCR1 expression define human CD11c$^+$CD141$^+$ cells as homologues of mouse CD8$^+$ dendritic cells. *J. Exp. Med.* 207: 1273–1281.
17. Haniffa, M., A. Shin, V. Bigley, N. McGovern, P. Teo, P. See, P. S. Wasan, X. N. Wang, F. Malinarich, B. Malleret, et al. 2012. Human tissues contain CD141^{hi} cross-presenting dendritic cells with functional homology to mouse CD103$^+$ nonlymphoid dendritic cells. *Immunity* 37: 60–73.
18. Robbins, S. H., T. Walzer, D. Dembélé, C. Thibault, A. Defays, G. Bessou, H. Xu, E. Vivier, M. Sellars, P. Pierre, et al. 2008. Novel insights into the relationships between dendritic cell subsets in human and mouse revealed by genome-wide expression profiling. *Genome Biol.* 9: R17.
19. Stock, A., S. Booth, and V. Cerundolo. 2011. Prostaglandin E_2 suppresses the differentiation of retinoic acid-producing dendritic cells in mice and humans. *J. Exp. Med.* 208: 761–773.
20. Miyara, M., Y. Yoshioka, A. Kitoh, T. Shima, K. Wing, A. Niwa, C. Parizot, C. Taflin, T. Heike, D. Valeyre, et al. 2009. Functional delineation and differentiation dynamics of human CD4$^+$ T cells expressing the FoxP3 transcription factor. *Immunity* 30: 899–911.
21. Iyoda, T., S. Shimoyama, K. Liu, Y. Omatsu, Y. Akiyama, Y. Maeda, K. Takahara, R. M. Steinman, and K. Inaba. 2002. The CD8$^+$ dendritic cell subset selectively endocytoses dying cells in culture and in vivo. *J. Exp. Med.* 195: 1289–1302.
22. Ito, T., M. Inaba, K. Inaba, J. Toki, S. Sogo, T. Iguchi, Y. Adachi, K. Yamaguchi, R. Amakawa, J. Valladeau, et al. 1999. A CD1a$^+$/CD11c$^+$ subset of human blood dendritic cells is a direct precursor of Langerhans cells. *J. Immunol.* 163: 1409–1419.
23. Penna, G., and L. Adorini. 2000. 1α,25-Dihydroxyvitamin D3 inhibits differentiation, maturation, activation, and survival of dendritic cells leading to impaired alloreactive T cell activation. *J. Immunol.* 164: 2405–2411.
24. Piemonti, L., P. Monti, M. Sironi, P. Fraticelli, B. E. Leone, E. Dal Cin, P. Allavena, and V. Di Carlo. 2000. Vitamin D_3 affects differentiation, maturation, and function of human monocyte-derived dendritic cells. *J. Immunol.* 164: 4443–4451.
25. Penna, G., S. Amuchastegui, N. Giarratana, K. C. Daniel, M. Vulcano, S. Sozzani, and L. Adorini. 2007. 1,25-Dihydroxyvitamin D_3 selectively modulates tolerogenic properties in myeloid but not plasmacytoid dendritic cells. *J. Immunol.* 178: 145–153.
26. Spiegl, N., S. Didichenko, P. McCaffery, H. Langen, and C. A. Dahinden. 2008. Human basophils activated by mast cell-derived IL-3 express retinaldehyde dehydrogenase-II and produce the immunoregulatory mediator retinoic acid. *Blood* 112: 3762–3771.
27. Mora, J. R., M. Iwata, and U. H. von Andrian. 2008. Vitamin effects on the immune system: vitamins A and D take centre stage. *Nat. Rev. Immunol.* 8: 685–698.
28. Barone, F. C., E. A. Irving, A. M. Ray, J. C. Lee, S. Kassis, S. Kumar, A. M. Badger, R. F. White, M. J. McVey, J. J. Legos, et al. 2001. SB 239063, a second-generation p38 mitogen-activated protein kinase inhibitor, reduces brain injury and neurological deficits in cerebral focal ischemia. *J. Pharmacol. Exp. Ther.* 296: 312–321.
29. Davis, M. I., J. P. Hunt, S. Herrgard, P. Ciceri, L. M. Wodicka, G. Pallares, M. Hocker, D. K. Treiber, and P. P. Zarrinkar. 2011. Comprehensive analysis of kinase inhibitor selectivity. *Nat. Biotechnol.* 29: 1046–1051.
30. Mora, J. R., G. Cheng, D. Picarella, M. Briskin, N. Buchanan, and U. H. von Andrian. 2005. Reciprocal and dynamic control of CD8 T cell homing by dendritic cells from skin- and gut-associated lymphoid tissues. *J. Exp. Med.* 201: 303–316.
31. Szatmari, I., A. Pap, R. Rühl, J.-X. Ma, P. A. Illarionov, G. S. Besra, E. Rajnavolgyi, B. Dezso, and L. Nagy. 2006. PPARγ controls CD1d expression by turning on retinoic acid synthesis in developing human dendritic cells. *J. Exp. Med.* 203: 2351–2362.
32. Chang, S.-Y., H.-R. Cha, J.-H. Chang, H.-J. Ko, H. Yang, B. Malissen, M. Iwata, and M.-N. Kweon. 2010. Lack of retinoic acid leads to increased langerin-expressing dendritic cells in gut-associated lymphoid tissues. *Gastroenterology* 138: 1468–1478, e1–e6.
33. Bastie, J. N., N. Balitrand, F. Guidez, I. Guillemot, J. Larghero, C. Calabresse, C. Chomienne, and L. Delva. 2004. 1α,25-Dihydroxyvitamin D3 transrepresses retinoic acid transcriptional activity via vitamin D receptor in myeloid cells. *Mol. Endocrinol.* 18: 2685–2699.
34. Jaensson, E., H. Uronen-Hansson, O. Pabst, B. Eksteen, J. Tian, J. L. Coombes, P.-L. Berg, T. Davidsson, F. Powrie, B. Johansson-Lindbom, and W. W. Agace. 2008. Small intestinal CD103$^+$ dendritic cells display unique functional properties that are conserved between mice and humans. *J. Exp. Med.* 205: 2139–2149.
35. Sigmundsdottir, H., J. Pan, G. F. Debes, C. Alt, A. Habtezion, D. Soler, and E. C. Butcher. 2007. DCs metabolize sunlight-induced vitamin D3 to 'program' T cell attraction to the epidermal chemokine CCL27. *Nat. Immunol.* 8: 285–293.
36. Zehnder, D., R. Bland, M. C. Williams, R. W. McNinch, A. J. Howie, P. M. Stewart, and M. Hewison. 2001. Extrarenal expression of 25-hydroxyvitamin d(3)-1 α-hydroxylase. *J. Clin. Endocrinol. Metab.* 86: 888–894.
37. Hewison, M. 2012. An update on vitamin D and human immunity. *Clin. Endocrinol.* 76: 315–325.
38. Iwata, M., Y. Eshima, and H. Kagechika. 2003. Retinoic acids exert direct effects on T cells to suppress Th1 development and enhance Th2 development via retinoic acid receptors. *Int. Immunol.* 15: 1017–1025.
39. Allen, J. E., and T. A. Wynn. 2011. Evolution of Th2 immunity: a rapid repair response to tissue destructive pathogens. *PLoS Pathog.* 7: e1002003.
40. Palm, N. W., R. K. Rosenstein, and R. Medzhitov. 2012. Allergic host defences. *Nature* 484: 465–472.
41. Chu, C.-C., N. Ali, P. Karagiannis, P. Di Meglio, A. Skowera, L. Napolitano, G. Barinaga, K. Grys, E. Sharif-Paghaleh, S. N. Karagiannis, et al. 2012. Resident CD141 (BDCA3)$^+$ dendritic cells in human skin produce IL-10 and induce regulatory T cells that suppress skin inflammation. *J. Exp. Med.* 209: 935–945.

OPEN ACCESS Freely available online

PLOS ONE

Moderate Restriction of Macrophage-Tropic Human Immunodeficiency Virus Type 1 by SAMHD1 in Monocyte-Derived Macrophages

Kahoru Taya, Emi E. Nakayama, Tatsuo Shioda*

Department of Viral Infections, Research Institute for Microbial Diseases, Osaka University, Suita, Osaka, Japan

Abstract

Macrophage-tropic human immunodeficiency virus type 1 (HIV-1) strains are able to grow to high titers in human monocyte-derived macrophages. However, it was recently reported that cellular protein SAMHD1 restricts HIV-1 replication in human cells of the myeloid lineage, including monocyte-derived macrophages. Here we show that degradation of SAMHD1 in monocyte-derived macrophages was associated with moderately enhanced growth of the macrophage-tropic HIV-1 strain. SAMHD1 degradation was induced by treating target macrophages with vesicular stomatitis virus glycoprotein-pseudotyped human immunodeficiency virus type 2 (HIV-2) particles containing viral protein X. For undifferentiated monocytes, HIV-2 particle treatment allowed undifferentiated monocytes to be fully permissive for productive infection by the macrophage-tropic HIV-1 strain. In contrast, untreated monocytes were totally resistant to HIV-1 replication. These results indicated that SAMHD1 moderately restricts even a macrophage-tropic HIV-1 strain in monocyte-derived macrophages, whereas the protein potently restricts HIV-1 replication in undifferentiated monocytes.

Citation: Taya K, Nakayama EE, Shioda T (2014) Moderate Restriction of Macrophage-Tropic Human Immunodeficiency Virus Type 1 by SAMHD1 in Monocyte-Derived Macrophages. PLoS ONE 9(3): e90969. doi:10.1371/journal.pone.0090969

Editor: Chen Liang, Lady Davis Institute for Medical Research, Canada

Received October 8, 2013; **Accepted** February 5, 2014; **Published** March 5, 2014

Funding: This work was supported by a grant from the Ministry of Education, Culture, Sports, Science, and Technology, and by a grant from the Ministry of Health, Labour and Welfare, Japan. The funders had no role in study design, data collection and analysis, decision to publish, or preparation of the manuscript.

Competing Interests: The authors have declared that no competing interests exist.

* E-mail: shioda@biken.osaka-u.ac.jp

Introduction

CD4 is the primary receptor molecule of human immunodeficiency virus type 1 (HIV-1) for viral attachment to the target cells [1]. HIV-1 thus replicates in $CD4^+$ cells such as activated human $CD4^+$ lymphocytes and macrophages [2,3]. Among different HIV-1 strains, macrophage-tropic HIV-1 strains replicate particularly well in cultured human monocyte-derived macrophages [4]. Many macrophage-tropic HIV-1 strains fail to replicate well in established human T cell lines such as Hut78 and MT4, cell lines in which laboratory-adapted T-cell line-tropic HIV-1 strains can replicate efficiently. Conversely, many laboratory-adapted T-cell line-tropic HIV-1 strains fail to replicate well in monocyte-derived macrophages [5]. Sequence variations in the HIV-1 envelope protein, especially in the third variable region, correlate with the HIV-1 cellular host range [6–9], and this observation led to the identification of the CCR5 and CXCR4 chemokine receptors as HIV-1 co-receptors for viral fusion with target cell membranes [10–16]. Macrophage-tropic HIV-1 strains utilize CCR5 as a co-receptor, and most such macrophage-tropic HIV-1 strains now have been re-designated as R5-tropic strains, although not all the R5-tropic HIV-1 strains can efficiently replicate in macrophages [17–19]. Laboratory-adapted T-cell line-tropic HIV-1 strains utilize CXCR4 as a co-receptor, and most such T-cell line-tropic HIV-1 strains now have been re-designated as X4-tropic strains, although CXCR4 expression also was observed in macrophages [20–22], cells in which X4-tropic strains cannot replicate well.

Despite the presence of the aforementioned HIV-1 strains that can replicate well in macrophages, it has been also reported that HIV-1-based lentivirus vectors composed of HIV-1 Gag and Pol proteins and vesicular stomatitis virus glycoprotein (VSV-G) showed markedly reduced efficiency for transduction of cells of myeloid lineage [23,24]. The restriction was rather strong in monocyte-derived dendritic cells and to a lesser extent in monocyte-derived macrophages [25,26]. Such a myeloid lineage-specific restriction was not observed in lentivirus vectors based on simian immunodeficiency virus isolated from macaques (SIVmac) [26], which is in the same lineage as human immunodeficiency virus type 2 (HIV-2), or in simian immunodeficiency virus isolated from sooty mangabey (SIVsm). The myeloid lineage-specific restriction of HIV-1-based lentivirus vector could also be abrogated by pretreatment of cells with SIVmac particles [27]. Members of HIV-2 and SIVsm lineage encode a non-structural viral protein X (Vpx) that is absent from HIV-1. VpX was shown to abrogate the myeloid lineage-specific restriction of HIV-1-basesd lentivirus vectors [27–29].

In 2011, SAMHD1 (a cellular protein SAM- and HD-domain-containing protein) was implicated as a target of Vpx that was responsible for abrogation of HIV-1 restriction in human cells of myeloid lineage [30,31]. Subsequently, SAMHD1 was shown to restrict HIV-1 infection in resting $CD4^+$ T cells [32]. SAMHD1 possesses deoxynucleoside triphosphate triphosphohydrolase activity; this activity reduces levels of deoxynucleoside triphosphate in cells of myeloid lineage and resting $CD4^+$ cells, thereby preventing reverse-transcription of HIV-1 RNA in these cell types

[33,34]. Vpx antagonizes SAMHD1 and induces proteolytic degradation of SAMHD1 through the CUL4A/DCAF1 E3 ubiquitin ligase complex [30].

In most of the SAMHD1 studies cited above, the efficiency of HIV-1 infection was assayed in the context of lentivirus vectors composed of HIV-1 Gag and Pol proteins packaged with VSV-G protein, along with reporter genes such as those encoding luciferase or green fluorescent protein. This distinction raises the question of whether SAMHD1 provides the same function in live HIV-1 viruses. Therefore, in the study presented here, we re-evaluated the role of SAMHD1 in HIV-1 replication in monocyte-derived macrophages in the context of a live macrophage-tropic HIV-1 strain that can replicate well in macrophages.

Results

Lack of Enhancing Effect of Macrophage-tropic HIV-1 Strain on HIV-1 Infection in Monocyte-derived Macrophages

SAMHD1 was reported to suppress infection of HIV-1-based lentivirus vectors containing VSV-G in cultured monocyte-derived macrophages [30]. On the other hand, macrophage-tropic HIV-1 strains can efficiently replicate in monocyte-derived macrophages [4]. To reconcile these potentially contradictory results, we tested the hypothesis that live macrophage-tropic HIV-1 strains can evade restriction of SAMHD1 by an unidentified mechanism. As a first step, we treated monocyte-derived macrophages with a macrophage-tropic HIV-1 strain SF162 before inoculation with VSV-G-pseudotyped lentivirus vector expressing luciferase (NL43-Luci/VSV-G). Results showed that pretreatment with SF162 failed to enhance subsequent infection by NL43-Luci/VSV-G in macrophages (Fig. 1A and 1B, left panels), whereas pretreatment with VSV-G-pseudotyped and Env-defective HIV-2 particles containing Vpx (GH123-Nhe/VSV-G) enhanced luciferase expression (Fig. 1A and 1B, left panels), as reported previously [30]. The effect of GH123-Nhe/VSV-G was more prominent in undifferentiated monocytes than in fully differentiated macrophages; a more than 200-fold increase of luciferase activity was observed by pretreatment of monocytes with GH123-Nhe/VSV-G (Fig. 1A and 1B, right panels). SF162 again failed to enhance subsequent infection by NL43-Luci/VSV-G in monocytes (Fig. 1A and 1B, right panels).

Enhancing Effect of VSV-G Pseudotyped HIV-2 Particles on Macrophage-tropic HIV-1 Strain in Monocyte-derived Macrophages

We next tested whether GH123-Nhe/VSV-G also could enhance replication of a macrophage-tropic HIV-1 strain in monocyte-derived macrophages. Fig. 2 shows the effects of GH123-Nhe/VSV-G on replication of SF162 in cultured macrophages that were differentiated from monocytes with granulocyte-macrophage colony stimulating factor (GM-CSF). SF162 replicated to titers corresponding to approximately 100 ng/ml of p24 core protein (Fig. 2A and 2B, left panels). Up to five-fold higher titers were detected in SF162-infected macrophages pretreated with GH123-Nhe/VSV-G (Fig. 2A and 2B, left panels). These results indicated that GH123-Nhe/VSV-G could enhance replication of macrophage-tropic HIV-1 in GM-CSF-differentiated macrophage cultures. In contrast, the T-cell line-tropic HIV-1 strain NL43 did not replicate at all in macrophages, regardless of the presence or absence of GH123-Nhe/VSV-G treatment (Fig. 2A and B, right panels).

Monocyte-derived macrophages differentiated with macrophage colony stimulating factor (M-CSF) are more susceptible to HIV-1 infection than those differentiated with GM-CSF [35–38]. We therefore tested whether GH123-Nhe/VSV-G could enhance SF162 replication in monocyte-derived macrophages differentiated with M-CSF. SF162 grew to titers corresponding to 200 ng/ml of p24 in donor 1 macrophages (Fig. 3A, left) and to 400 ng/ml of p24 in donor 2 macrophages (Fig. 3B, left), a level at least two-fold higher than those found in SF162-infected macrophage cultures differentiated with GM-CSF. Up to five-fold higher titers of SF162 also were detected in M-CSF-differentiated macrophage cultures pretreated with GH123-Nhe/VSV-G (Fig. 3A and 3B, left panels). These results indicated that GH123-Nhe/VSV-G could enhance replication of macrophage-tropic HIV-1 replication even in M-CSF-differentiated macrophages. The T-cell line-tropic NL43 strain again did not replicate at all in M-CSF-differentiated macrophages, regardless of the presence or absence of GH123-Nhe/VSV-G treatment (Fig. 3A and 3B, right panels).

Enhancing Effect of VSV-G-pseudotyped HIV-2 Particles on Macrophage-tropic HIV-1 Strain in Undifferentiated Monocytes

In contrast to differentiated macrophages, undifferentiated monocytes are highly resistant to HIV-1 infection, but treatment with GH123-Nhe/VSV-G greatly enhanced VSV-G-pseudotyped lentivirus vector transduction (Fig. 1A and 1B, right panels). This pattern also was observed for live SF162 infection of undifferentiated monocytes (Fig. 4 and 5). SF162 replication in monocytes was not observed until 12 days after infection, when cell morphology suggested that some of the monocytes in the culture had differentiated into macrophages. On the other hand, GH123-Nhe/VSV-G rendered cultured monocytes fully permissive for SF162 replication (Fig. 4A and 4B, left panels). Up to 50-fold higher titers of SF162 were detected in monocytes treated with GH123-Nhe/VSV-G than in untreated monocytes. Consistently, large multi-nucleated syncytia were observed 6 days after infection, but only in monocytes treated with GH123-Nhe/VSV-G (Fig. 5). These results are in good agreement with recent findings that non-stimulated $CD14^+$ cells obtained from Aicardi-Goutieres syndrome patients (who are homozygous for a nonsense mutation in the SAMHD1-encoding gene) were highly susceptible to macrophage-tropic HIV-1 infection [39]. As with GM-CSF- and M-CSF-differentiated macrophages, the T-cell line-tropic NL43 strain did not replicate at all in undifferentiated monocytes, regardless of the presence or absence of GH123-Nhe/VSV-G treatment (Fig. 4A and 4B, right panels).

Levels of SAMHD1 Expression in Monocytes and Macrophages

Vpx was reported to induce proteolytic degradation of SAMHD1. We therefore compared levels of SAMHD1 protein expression in cells treated with GH123-Nhe/VSV-G and those without treatment. As shown in Fig. 6, GH123-Nhe/VSV-G markedly reduced levels of SAMHD1 protein expression in monocytes and macrophages. Consistent with the previous observation [31], levels of SAMHD1 protein expression were apparently higher in undifferentiated monocytes than in macrophages.

We then quantitated levels of SAMHD1 mRNA expression in monocytes and macrophages. As expected, SAMHD1 mRNA levels were higher in monocytes than in macrophages (Fig. 7). There was no difference in SAMHD1 mRNA levels between cells treated with GH123-Nhe/VSV-G and those without treatment.

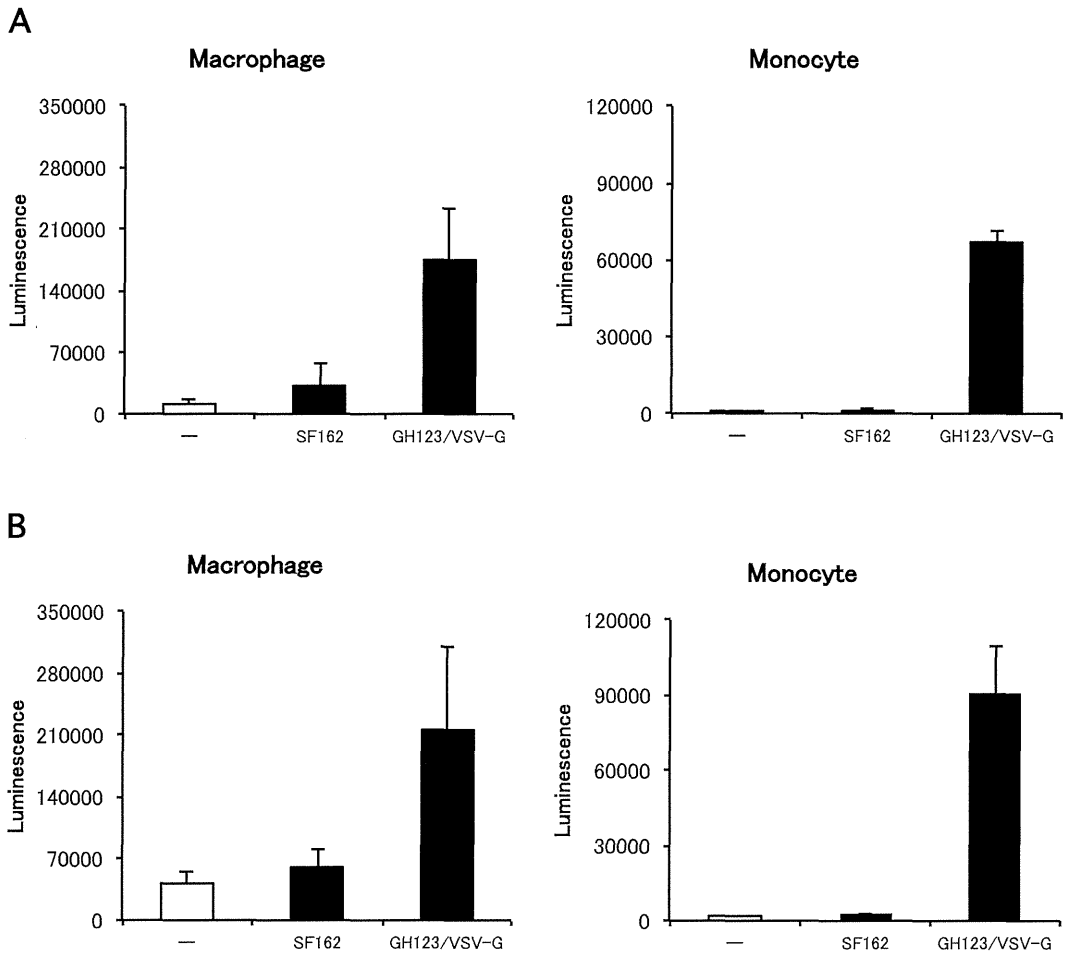

Figure 1. Effects of macrophage-tropic HIV-1 strain and VSV-G-pseudotyped HIV-2 particles on lentivirus vector infection. Monocytes were differentiated into macrophages for 11 days in the presence of GM-CSF. Macrophages or monocytes were treated with macrophage-tropic HIV-1 strain (SF162) or VSV-G pseudotyped and Env-defective HIV-2 particles (GH123/VSV-G) and then infected with lentivirus vector NL43-Luci/VSV-G. Luciferase activity was measured 4 days after infection. Data are plotted as the mean ± SD of triplicate samples; presented data are representative of three independent experiments using two donors. A: Results of samples obtained from a donor 1. B: Results of samples obtained from a donor 2.
doi:10.1371/journal.pone.0090969.g001

These results confirmed that reduced SAMHD1 protein levels in cells treated with GH123-Nhe/VSV-G were caused by enhanced degradation of SAMHD1 by HIV-2 particles containing Vpx.

Phosphorylation of SAMHD1 in Monocytes and Differentiated Macrophages

It was recently reported that Cyclin A2/CDK1 phosphorylates SAMHD1 at the threonine 592 residues. Phosphorylation of the SAMHD1 threonine 592 correlates with loss of its ability to restrict HIV-1 [40–42]. We therefore analyzed the phosphorylation state of SAMHD1 in monocytes and differentiated macrophages. As shown in Fig. 8, SAMHD1 proteins in monocytes were less phosphorylated than those in GM-CSF-differentiated or M-CSF-differentiated macrophages. This result is in good agreement with those reported previously [40], and correlated well with our results that SAMHD1 restriction in monocytes was much more potent than that in differentiated macrophages (Fig. 1 and 4). Treatment with GH123-Nhe/VSV-G reduced both phosphorylated and nonphosphorylated SAMHD1 in all cells. There was no difference in the phosphorylation state of SAMHD1 between GM-CSF-differentiated and M-CSF-differentiated macrophages (Fig. 8).

Enhancing Effect of SAMHD1 siRNA on HIV-1 Infection in Monocytes and Monocyte-derived Macrophages

To confirm that the observed enhancing effect of VSV-G-pseudotyped HIV-2 particles on HIV-1 infection was due to degradation of SAMHD1 in monocytes and macrophages, we used siRNAs targeting SAMHD1 to reduce levels of SAMHD1 expression. The siRNAs targeting SAMHD1 reduced levels of SAMHD1 mRNA in both monocytes and GM-CSF-differentiated macrophages (Fig. 9A and 9B, left panels). Accordingly, increased levels of NL43-Luci/VSV-G infection were observed in monocytes (Fig. 9A and 9B, middle panels) and GM-CSF-differentiated macrophages (Fig. 9A and 9B, right panels) transfected with the siRNAs targeting SAMHD1. These results confirmed that the enhancing effect of VSV-G-pseudotyped HIV-2 particles on HIV-1 infection was due to degradation of SAMHD1.

Discussion

SAMHD1 was reported to suppress HIV-1 infection of cells of myeloid lineage, including monocyte-derived macrophages [30,31]. Nevertheless, macrophage-tropic HIV-1 strains can efficiently replicate in monocyte-derived macrophages [4,6–8].

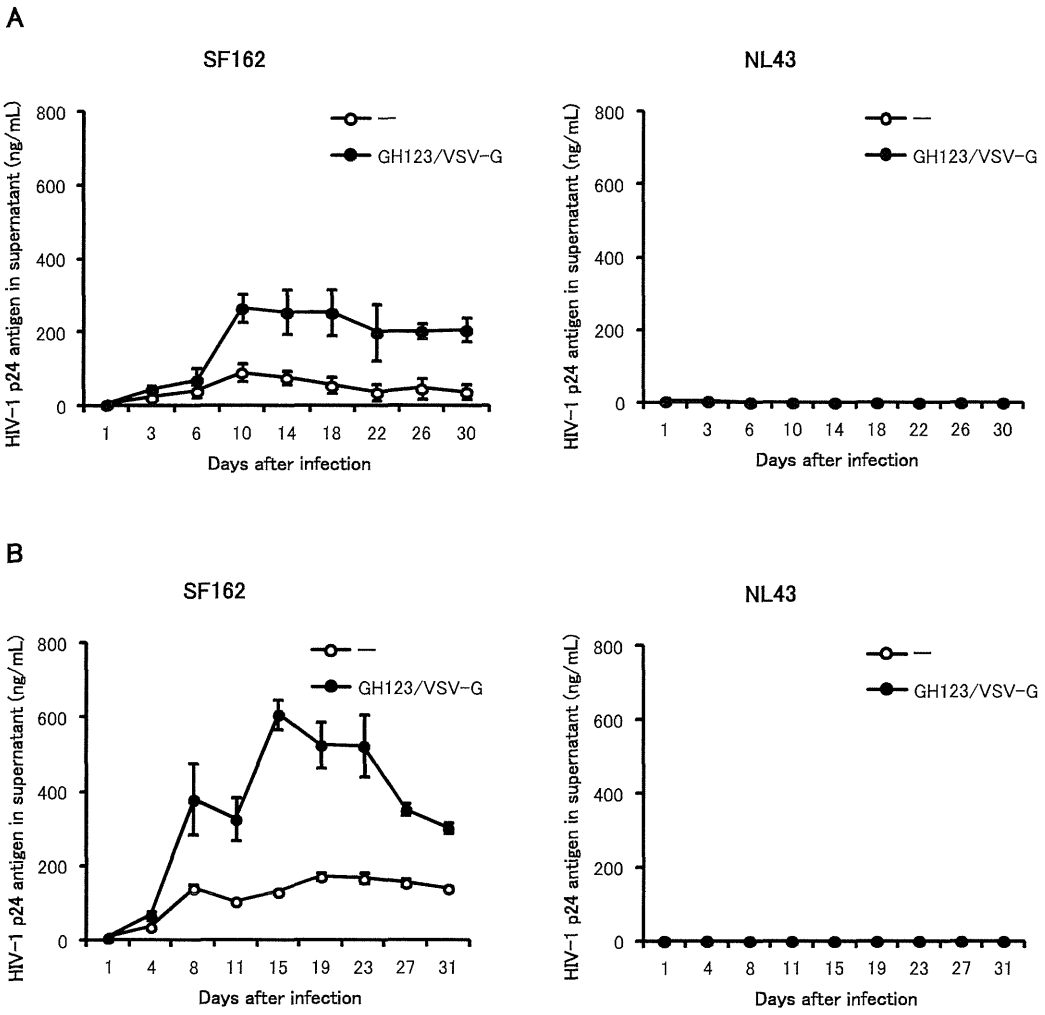

Figure 2. Effects of VSV-G-pseudotyped HIV-2 particles on macrophage-tropic and T-cell line-tropic HIV-1 strains in GM-CSF-induced macrophages. Monocytes were differentiated into macrophages for 6 days in the presence of GM-CSF. Macrophages were treated with VSV-G pseudotyped and Env-defective HIV-2 particles (GH123/VSV-G) and then infected with HIV-1 strain SF162 or NL43. HIV-1 replication was quantified by ELISA measurement of p24 antigen in the supernatant after infection. Data are plotted as the mean ± SD of triplicate samples; presented data are representative of three independent experiments using two donors. A: Results of samples obtained from a donor 1. B: Results of samples obtained from a donor 2.
doi:10.1371/journal.pone.0090969.g002

In the present study, we have shown that the treatment of monocyte-derived macrophages or undifferentiated monocytes with GH123-Nhe/VSV-G enhanced subsequent macrophage-tropic HIV-1 infection. GH123-Nhe/VSV-G treatment reduced levels of SAMHD1 protein expression in monocyte-derived macrophages and undifferentiated monocytes. Enhancing effects by GH123-Nhe/VSV-G were observed even in M-CSF-induced monocyte-derived macrophages, which were reported to be highly susceptible to HIV-1 infection [35–38,43]. These results indicated that SAMHD1 could moderately suppress replication of the macrophage-tropic HIV-1 strain in monocyte-derived macrophages. It is formally possible that live macrophage-tropic HIV-1 strains evade restriction of SAMHD1 by an unidentified mechanism, although we consider such a possibility unlikely.

Levels of HIV-1 restriction by SAMHD1 in monocyte-derived macrophages were rather modest, while those in undifferentiated monocytes were quite strong (Fig. 2, 3 and 4). SAMHD1 expression levels were higher in undifferentiated monocytes than in monocyte-derived macrophages (Fig. 6 and 7), showing a clear correlation between levels of SAMHD1 expression and those of restriction. Furthermore, phosphorylation of SAMHD1, which was reported to abolish HIV-1 restriction activity of SAMHD1 [40–42], was more prominent in M-CSF-induced or GM-CSF-induced macrophages than in undifferentiated monocytes (Fig. 8). When we compared M-CSF-induced and GM-CSF-induced macrophages, HIV-1 grew to higher titers in M-CSF-induced macrophages than in GM-CSF-induced macrophages. This result is in good agreement with those of the previous studies [37,43]. The levels of restriction by SAMHD1 also were slightly lower in M-CSF-induced macrophages than in GM-CSF-induced macrophages, although we failed to observe clear differences in levels of expression or phosphorylation state of SAMHD1 between M-CSF-induced and GM-CSF-induced macrophages (Fig. 6, 7, and 8). Thus, mechanisms underlying the higher sensitivity to HIV-1 infection in M-CSF-induced macrophages are not clear at present; further studies are necessary, including comparisons of CD4 and CCR5 expression levels between M-CSF-induced and GM-CSF-induced macrophages.

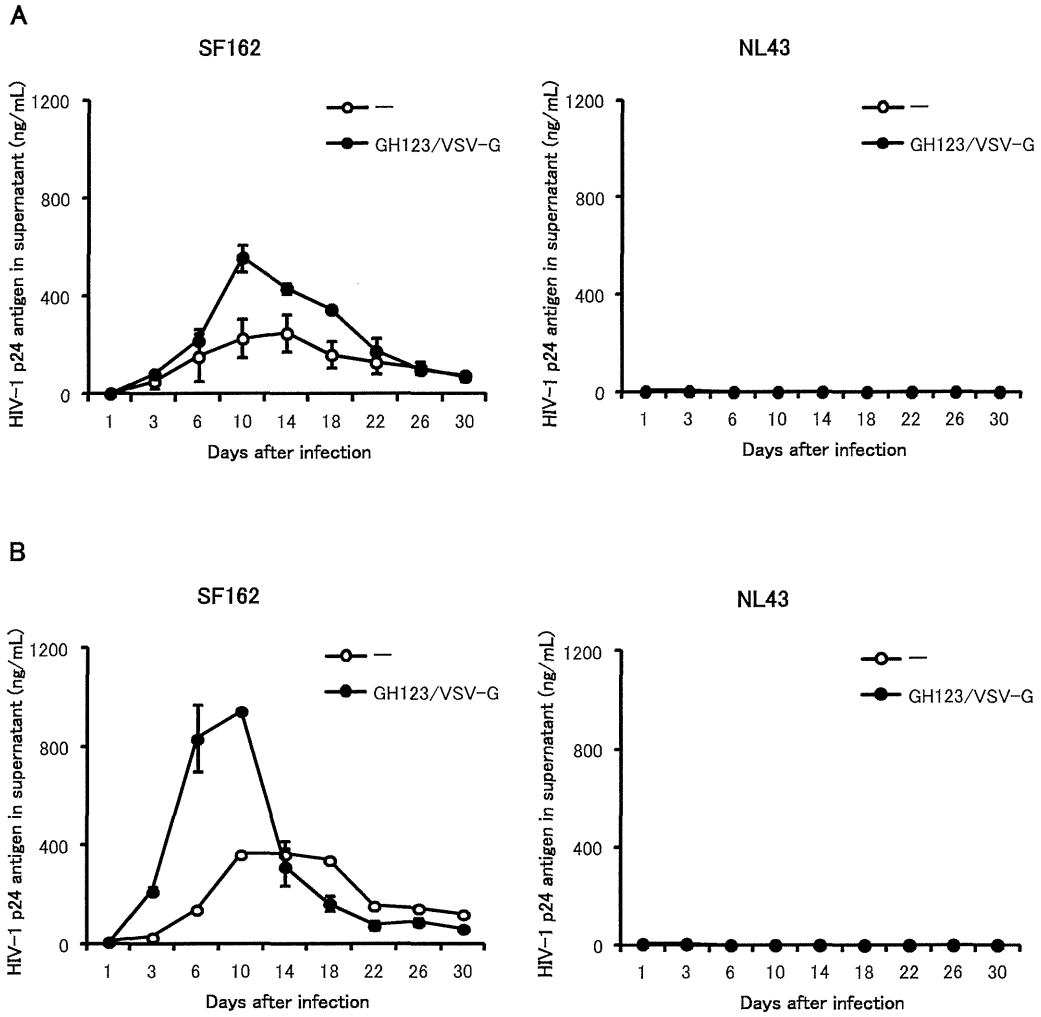

Figure 3. Effects of VSV-G-pseudotyped HIV-2 particles on macrophage-tropic and T-cell line-tropic HIV-1 strains in M-CSF-induced macrophages. Monocytes were differentiated into macrophages for 6 days in the presence of M-CSF. Macrophages were treated with VSV-G pseudotyped and Env-defective HIV-2 particles (GH123/VSV-G) and then infected with HIV-1 strain SF162 or NL43. HIV-1 replication was quantified by ELISA measurement of p24 antigen in the supernatant after infection. Data are plotted as the mean ± SD of triplicate samples; presented data are representative of two independent experiments using two donors. A: Results of samples obtained from a donor 1. B: Results of samples obtained from a donor 2.
doi:10.1371/journal.pone.0090969.g003

It should be noted here that the effects of GH123-Nhe/VSV-G treatment seem to last relatively long, although we treated cells only once with GH123-Nhe/VSV-G. It is possible that the Vpx protein produced by the transduced HIV-2 genomes was incorporated into infectious SF162 progeny virions and thus facilitated replication of SF162 in the next cycle of infection. It is also possible that Env-deficient progeny HIV-2 virions were pseudotyped with fully functional SF162 envelope proteins, and thereby continued to produce Vpx that degraded SAMHD1.

Similar to monocytes and macrophages, microglial cells in the human brain are derived via the myeloid lineage and are also susceptible to HIV-1 infection [44]. HIV-1-infected microglial cells appear to play an important role in HIV-1-associated neurological disorders such as dementia and neurocognitive disorder [45]. It therefore would be interesting to investigate whether or not SAMHD1 moderately suppresses HIV-1 replication in microglial cells just as in macrophages. If SAMHD1 can suppress HIV-1 replication at least moderately in microglial cells, artificial potentiation of SAMHD1 in microglial cells might be a novel approach to the treatment of HIV-1-associated neurological disorders.

In conclusion, we have shown that SAMHD1 moderately restricts even macrophage-tropic HIV-1 strains in monocyte-derived macrophages. SAMHD1 restriction was much more potent in undifferentiated monocytes than that in GM-CSF-differentiated or M-CSF-differentiated macrophages. Levels of expression and phosphorylation state of SAMHD1 could at least partially explain the different levels of SAMHD1 restriction between undifferentiated monocytes and differentiated macrophages.

Materials and Methods

Ethics Statement

Peripheral blood mononuclear cells (PBMC) were obtained from healthy donors with written informed consent. Use of human

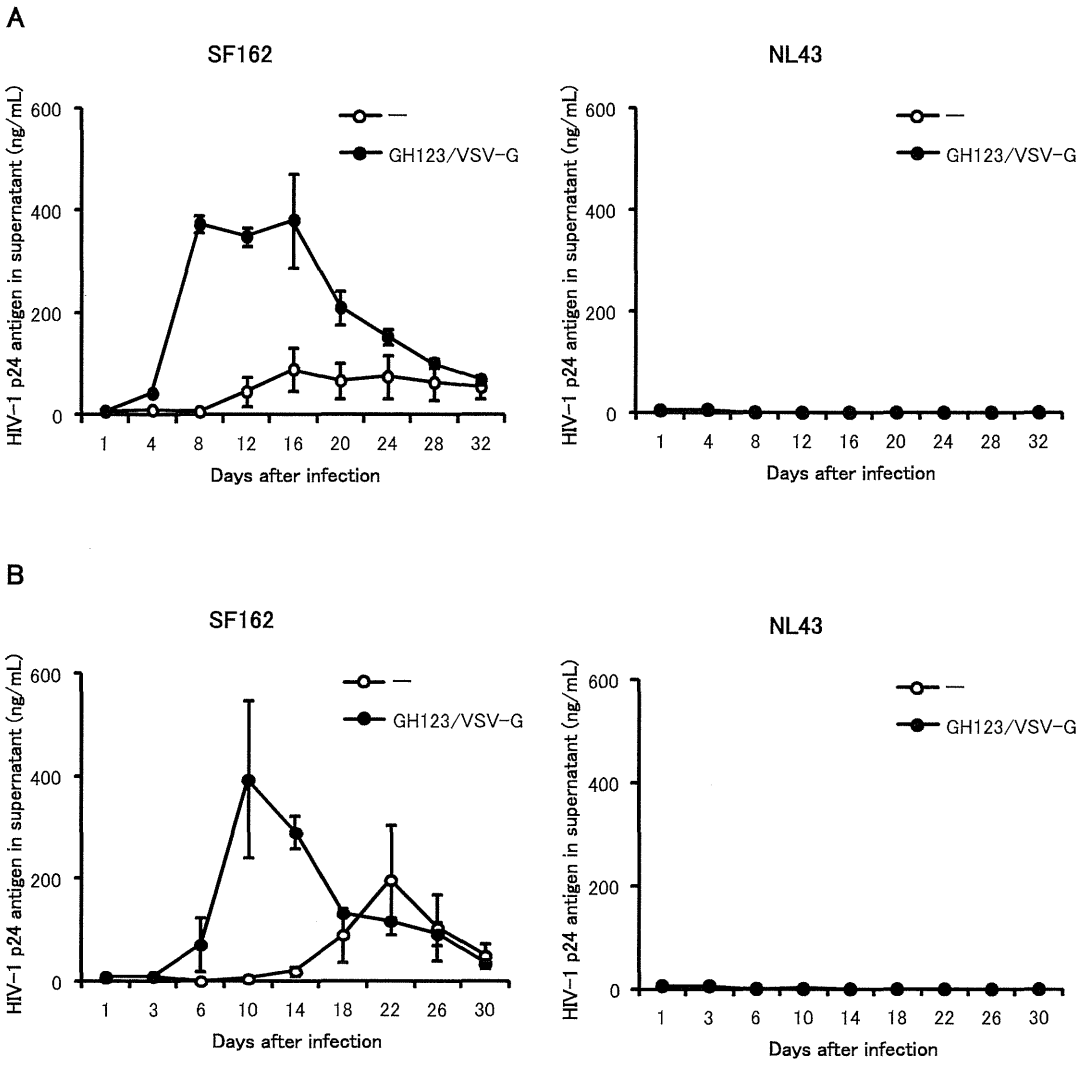

Figure 4. Effects of VSV-G-pseudotyped HIV-2 particles on macrophage-tropic and T-cell line-tropic HIV-1 strains in undifferentiated monocytes. Monocytes were treated with VSV-G pseudotyped and Env-defective HIV-2 particles (GH123/VSV-G) and then infected with HIV-1 strain SF162 or NL43. HIV-1 replication was quantified by ELISA measurement of p24 antigen in the supernatant after infection. Data are plotted as the mean ± SD of triplicate samples obtained from a single blood donor; presented data are representative of three independent experiments using two donors. A: Results of samples obtained from a donor 1. B: Results of samples obtained from a donor 2.
doi:10.1371/journal.pone.0090969.g004

materials in this study was approved by the Research Ethics Committee of Osaka University.

Viruses

Macrophage-tropic HIV-1 strain SF162 and laboratory-adapted T-cell line-tropic HIV-1 strain NL43 were grown in CCR5-expressing MT4 cells [46] and titrated for use with the RETROtek Antigen ELISA kit (ZeptoMetrix, Buffalo, NY). VSV-G-pseudotyped lentivirus vector expressing luciferase (NL43-Luci/VSV-G) and VSV-G-pseudotyped and Env-defective HIV-2 particles containing Vpx (GH123-Nhe/VSV-G) were produced from human embryonic kidney cells (293T cells) using polyethylenimine (PEI) (molecular weight, 25,000; Polysciences, Warrington, PA). Briefly, for NL43-Luci/VSV-G virus production, 293T cells were transfected with 15 μg of pNL4-3-Luc-R-E- plasmid and 5 μg of VSV-G-encoding plasmid; for GH123-Nhe/VSV-G virus production, 293T cells were transfected with 15 μg of GH123-Nhe and 5 μg of VSV-G-encoding plasmid. The GH123-Nhe plasmid was generated by blunting the *Nhe*I site in the HIV-2 GH123 plasmid, thereby introducing a frame-shift mutation in its *env* gene. For transfected cells, medium was replaced 6 h after transfection, and viruses were harvested 48 h later. Viral titers were measured with the RETROtek Antigen ELISA kit.

Cells

PBMCs were obtained from blood buffy coats of healthy donors using Ficoll-Paque density gradient centrifugation, and then plated in 24-well, 12-well, or 6-well MULTIWELL PRIMARIA plates (Becton Dickinson, Franklin Lakes, NJ) with RPMI 1640 supplemented with 10% fetal calf serum (FCS). To obtain the monocyte population, the floating cells were removed by washing the plates with phosphate-buffered saline (PBS) four times after incubation at 37°C for 1 day. Monocytes were differentiated into macrophages for 6–11 days in the presence of 100 ng/ml of granulocyte macrophage colony stimulating factor (GM-CSF)

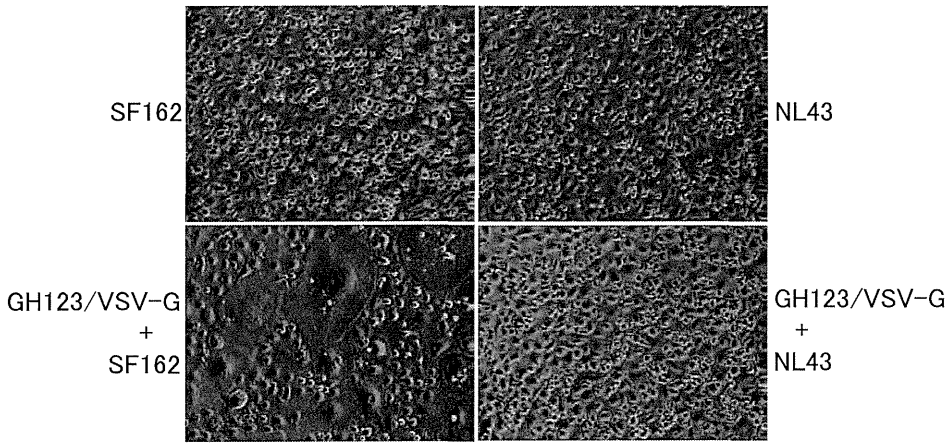

Figure 5. Syncytium formation in undifferentiated monocytes pretreated with HIV-2 particles and then infected with macrophage-tropic HIV-1. Monocytes were treated with VSV-G pseudotyped and Env-defective HIV-2 particles (GH123/VSV-G) and then infected with HIV-1 strain SF162 or NL43. Presented data are representative of two independent experiments.
doi:10.1371/journal.pone.0090969.g005

(PeproTECH, Rocky Hill, NJ) or 100 ng/ml of macrophage colony stimulating factor (M-CSF) (PeproTECH).

Luciferase Assay

Macrophages ($1.6–2.4\times10^5$ cells) and monocytes ($2.6–3.4\times10^6$ cells) were pretreated for 2 h with a titer of macrophage-tropic HIV-1 strain SF162 virus equivalent to 100 ng of p24 or with a titer of GH123-Nhe/VSV-G virus equivalent to 100 ng of p27, and then infected with a titer of NL43-Luci/VSV-G virus equivalent to 7.7 ng of p24. After incubation for 2 h, the medium was changed, and cells were incubated for 4 days at 37°C. Luciferase activity was measured in cell lysates according to the manufacturer's instructions (Bright-Glo Luciferase Assay System, Promega, Madison, WI) and read using a Centro LB960 Microplate Luminometer (Berthold, Bad Wildbad, Germany).

Virus Infection

Macrophages and monocytes ($2.2–2.6\times10^6$ cells) were pretreated for 2 h with a titer of GH123-Nhe/VSV-G virus equivalent to 100 ng of p27, and then infected with a titer of virus equivalent to 100 ng of p24 of macrophage-tropic HIV-1 strain SF162 or laboratory-adapted T-cell line-tropic HIV-1 strain NL43. After incubation for 2 h, cells were washed with PBS and incubated with RPMI 1640 supplemented with 10% FCS and 100 ng/ml GM-CSF or 100 ng/ml M-CSF. Culture supernatants were collected periodically, and levels of HIV-1 p24 antigen were measured by the RETROtek HIV-1 p24 Antigen ELISA kit.

Western Blot

Monocytes and macrophages (3.5×10^6 cells) were lysed in Laemmli sample buffer (100 mM Tris-HCl, pH 6.8, 0.04% sodium dodecyl sulfate (SDS), 20% glycerol, 0.12% 2-mercapto-ethanol). Proteins in the lysates were subjected to SDS-polyacryl-amide gel electrophoresis (SDS-PAGE). Proteins in the gel were

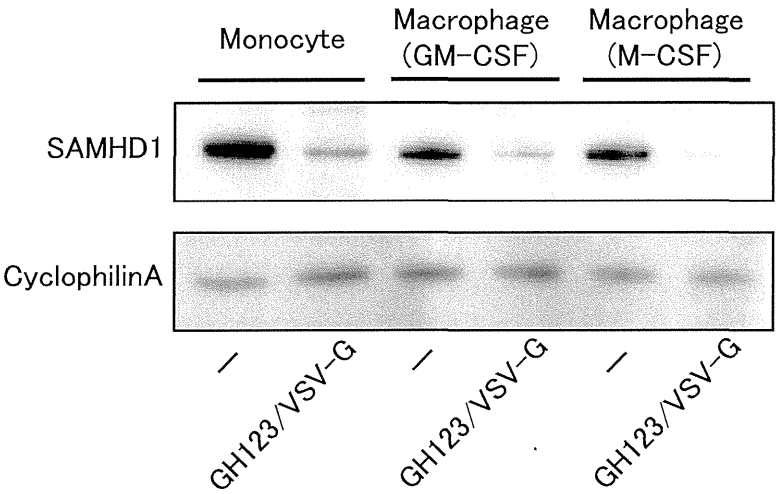

Figure 6. Western blot analysis of SAMHD1 in undifferentiated monocytes and macrophages. Monocytes were differentiated into macrophages for 6 days in the presence of GM-CSF or M-CSF. Macrophages or monocytes were treated with or without VSV-G-pseudotyped and Env-defective HIV-2 particles (GH123/VSV-G), and harvested. Whole-cell extracts were separated on SDS-PAGE and analyzed by western blot using the indicated antibodies. Presented data are representative of two independent experiments.
doi:10.1371/journal.pone.0090969.g006

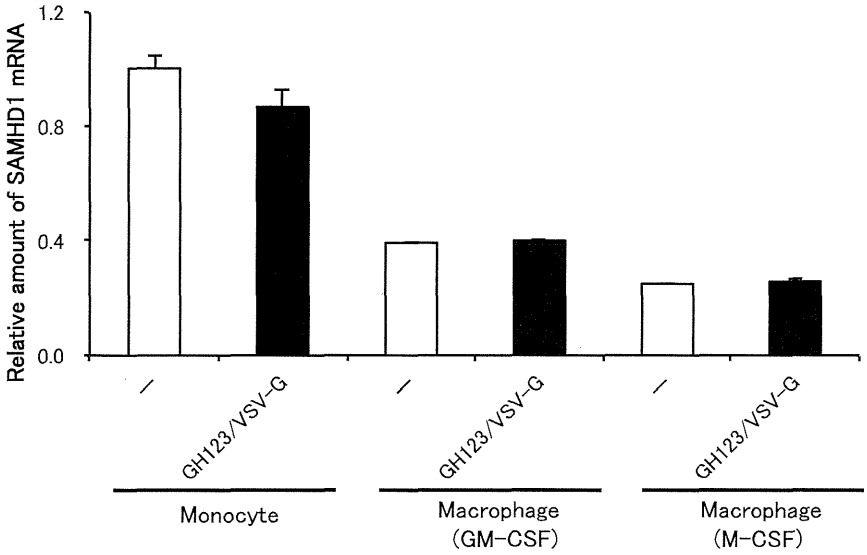

Figure 7. Quantification of SAMHD1 mRNA expression. Monocytes were differentiated into macrophages for 6 days in the presence of GM-CSF or M-CSF. Macrophages or monocytes were treated with or without VSV-G-pseudotyped and Env-defective HIV-2 particles (GH123/VSV-G), and harvested. SAMHD1 mRNA expression levels were detected by real-time RT-PCR and normalized against GAPDH. Data are shown as mean ± SD.
doi:10.1371/journal.pone.0090969.g007

then electrically transferred to a membrane (Immobilion; Millipore, Billerica, MA). Blots were blocked and probed with anti-CypA affinity rabbit polyclonal antibody (Sigma, St. Louis, MO) overnight at 4°C. Blots then were incubated with peroxidase-linked protein A (GE Healthcare, Buckinghamshire, UK), and bound antibodies were visualized with a Chemilumi-One chemiluminescent kit (Nacalai Tesque, Kyoto, Japan). Quantities of cell lysate were normalized by CypA level, then subjected to a new round of SDS-PAGE and membrane transfer. For the new blot, SAMHD1 protein in the membrane was detected with anti-SAMHD1 (611–625) rabbit antibody (Sigma) followed by peroxidase-linked protein A (GE Healthcare, Buckinghamshire, UK) detection as described above.

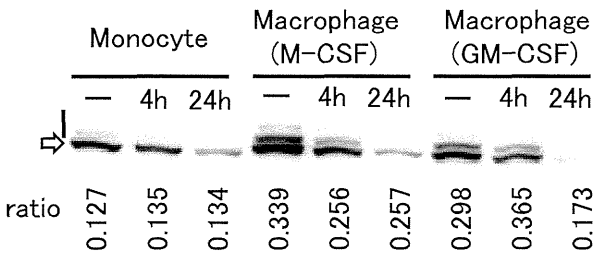

Figure 8. Phosphorylation state of SAMHD1. Monocytes (Monocyte), M-CSF-differentiated macrophages (Macrophage (M-CSF)), and GM-CSF-differentiated macrophages (Macrophage (GM-CSF)) were treated with GH123-Nhe/VSV-G for 2 h and incubated at 37°C for 4 h (4 h) or 24 h (24 h), or mock-treated (−). Cells were lyzed and subjected for SDS-PAGE containing Phos-tag to separate phosphorylated proteins from nonphosphorylated ones. SAMHD1 proteins were detected by anti-SAMHD1 antibody. Upper bands shown by a vertical bar and a lower band shown by an arrow represent phosphorylated and nonphosphorylated SAMHD1, respectively. Ratios of phosphorylated SAMHD1 levels to total SAMHD1 levels (ratio) are shown in vertical numbers.
doi:10.1371/journal.pone.0090969.g008

Phosphorylation State of SAMHD1

Monocyte or macrophages (6×10^6 cells) were treated with a titer of GH123-Nhe/VSV-G virus equivalent to 500 ng of p25 for 2 h, washed with medium, and then incubated at 37°C for 4 h or 24 h. Cells were lysed in Laemmli sample buffer. Proteins in the lysates were separated by SDS-PAGE containing Phos-tag (Wako, Osaka, Japan), a ligand that decreases the mobility of phosphorylated proteins. Separated proteins in the gel were analyzed by western blotting using anti-SAMHD1 antibody. The gel images were analyzed by CS analyzer 3.0 (ATTO, Tokyo, Japan).

Quantification of SAMHD1 mRNA Expression

Total RNA was extracted from monocytes or macrophages using TRIZOL reagent (Life Technologies, Carlsbad, CA) following the manufacturer's instructions. cDNA was synthesized from 1 μg of total RNA using the High-capacity cDNA Archive kit (Applied Biosystems, Carlsbad, CA) according to the manufacturer's instructions. For real time PCR, each 20-μL reaction mixture consisted of 5 μL of cDNA, 10 μL TaqMan Universal PCR Master Mix (Applied Biosystems, Carlsbad, CA) and 1 μL of TaqMan Gene Ex Assays (Assay ID: Hs00210019_m1). Real time PCR was performed with an Applied Biosystems 7500 Real-Time PCR System. Levels of SAMHD1 mRNA were normalized with those of GAPDH according to the manufacturer's instructions.

RNA Interference

The cultured medium of monocytes ($1.6–2.4\times10^6$ cells) was replaced with 0.5 mL of Opti-MEM (Gibco, Carlsbad, CA) before transfection. The SAMHD1-targeting pool comprised of the siRNAs to the following target sequences: J-013950-09: 5′-GACAAUGAGUUGCGUAUUU-3′; J-013950-10: 5′-CAUGUUUGAUGGACGAUUU-3′; J-013950-11: 5′-AAGUAUUGCUAGACGUGAA-3′; J-013950-12: 5′-UUAGUUAUAUCCAGCGAUU-3′ were purchased from Dharmacon (Lafayette, CO). The GFP-targeting siRNA to the sequence 5′-GGCTACGTCCAGGAGCGCACC-3′ were used as a control siRNA. Monocytes were transfected with 40 pmol aliquots of siRNA with 2 μL of Lipofectamine 2000 (Invitrogen, Carlsbad,

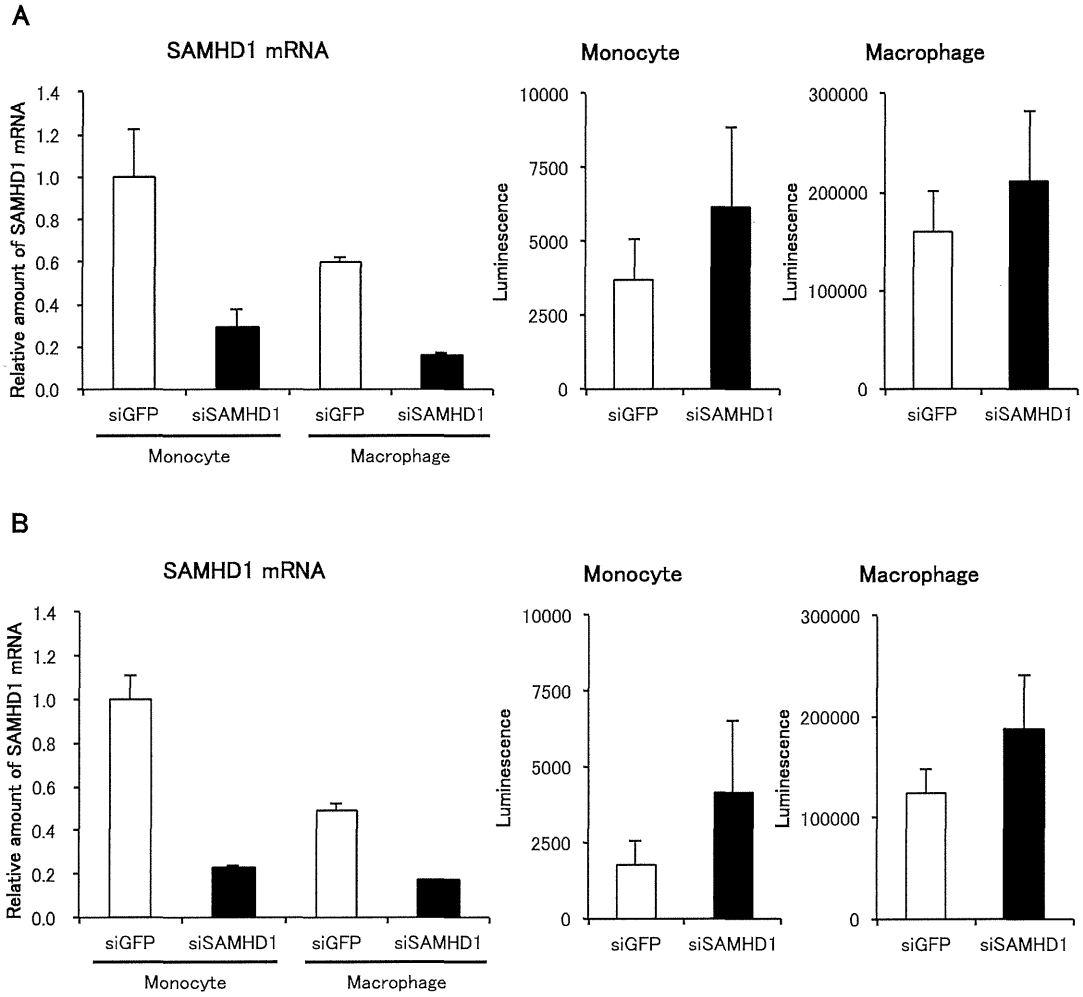

Figure 9. Effects of SAMHD1 siRNA on HIV-1 infection. Monocytes (Monocyte) or macrophages (Macrophage) were treated with SAMHD1- (siSAMHD1) or GFP- (siGFP) targeting siRNAs. Three days after transfection, cells were harvested or infected with NL43-Luci/VSV-G virus. SAMHD1 mRNA expression levels in harvested cells were detected by real-time RT-PCR and normalized against GAPDH. Data are shown as mean ± SD. Luciferase activity in infected cells was measured 4 days after infection. Data are plotted as the mean ± SD of triplicate samples; presented data are representative of two independent experiments using two donors. A: Results of samples obtained from a donor 1. B: Results of samples obtained from a donor 2.
doi:10.1371/journal.pone.0090969.g009

CA) per well. Six h after transfection, cultured medium was replaced with RPMI 1640 supplemented with 10% FCS. At day 3, monocytes were infected with a titer of NL43-Luci/VSV-G virus equivalent to 7.7 ng of p24. In the case of GM-CSF-induced macrophages ($1.6–3.6\times10^6$ cells), siRNAs were transfected at day 4 after differentiation by GM-CSF, and then infected with NL43-Luci/VSV-G virus at day 7. Total RNA was extracted from cells at the time point of NL43-Luci/VSV-G virus infection for quantification of SAMHD1 mRNA expression.

Acknowledgments

We are grateful to Dr. Tetsuro Matano for his critical discussion of this study. We thank Ms. Noriko Teramoto for her assistance. pNL4-3-Luc-R-E- plasmid was obtained through the AIDS Research and Reference Reagent Program, Division of AIDS, NIAID, NIH.

Author Contributions

Conceived and designed the experiments: EEN TS. Performed the experiments: KT EEN. Analyzed the data: KT EEN TS. Wrote the paper: KT EEN TS.

References

1. Maddon PJ, Dalgleish AG, McDougal JS, Clapham PR, Weiss RA, et al. (1986) The T4 gene encodes the AIDS virus receptor and is expressed in the immune system and the brain. Cell 47: 333–348.
2. Gartner S, Markovits P, Markovitz DM, Kaplan MH, Gallo RC, et al. (1986) The role of mononuclear phagocytes in HTLV-III/LAV infection. Science 233: 215–219.
3. Koenig S, Gendelman HE, Orenstein JM, Dal Canto MC, Pezeshkpour GH, et al. (1986) Detection of AIDS virus in macrophages in brain tissue from AIDS patients with encephalopathy. Science 233: 1089–1093.
4. Cheng-Mayer C, Weiss C, Seto D, Levy JA (1989) Isolates of human immunodeficiency virus type 1 from the brain may constitute a special group of the AIDS virus. Proc Natl Acad Sci U S A 86: 8575–8579.
5. Cheng-Mayer C, Seto D, Tateno M, Levy JA (1988) Biologic features of HIV-1 that correlate with virulence in the host. Science 240: 80–82.
6. Hwang SS, Boyle TJ, Lyerly HK, Cullen BR (1991) Identification of the envelope V3 loop as the primary determinant of cell tropism in HIV-1. Science 253: 71–74.

7. O'Brien WA, Koyanagi Y, Namazie A, Zhao JQ, Diagne A, et al. (1990) HIV-1 tropism for mononuclear phagocytes can be determined by regions of gp120 outside the CD4-binding domain. Nature 348: 69–73.
8. Shioda T, Levy JA, Cheng-Mayer C (1991) Macrophage and T cell-line tropisms of HIV-1 are determined by specific regions of the envelope gp120 gene. Nature 349: 167–169.
9. Shioda T, Levy JA, Cheng-Mayer C (1992) Small amino acid changes in the V3 hypervariable region of gp120 can affect the T-cell-line and macrophage tropism of human immunodeficiency virus type 1. Proc Natl Acad Sci U S A 89: 9434–9438.
10. Alkhatib G, Combadiere C, Broder CC, Feng Y, Kennedy PE, et al. (1996) CC CKR5: a RANTES, MIP-1alpha, MIP-1beta receptor as a fusion cofactor for macrophage-tropic HIV-1. Science 272: 1955–1958.
11. Berson JF, Long D, Doranz BJ, Rucker J, Jirik FR, et al. (1996) A seven-transmembrane domain receptor involved in fusion and entry of T-cell-tropic human immunodeficiency virus type 1 strains. J Virol 70: 6288–6295.
12. Choe H, Farzan M, Sun Y, Sullivan N, Rollins B, et al. (1996) The beta-chemokine receptors CCR3 and CCR5 facilitate infection by primary HIV-1 isolates. Cell 85: 1135–1148.
13. Deng H, Liu R, Ellmeier W, Choe S, Unutmaz D, et al. (1996) Identification of a major co-receptor for primary isolates of HIV-1. Nature 381: 661–666.
14. Doranz BJ, Rucker J, Yi Y, Smyth RJ, Samson M, et al. (1996) A dual-tropic primary HIV-1 isolate that uses fusin and the beta-chemokine receptors CKR-5, CKR-3, and CKR-2b as fusion cofactors. Cell 85: 1149–1158.
15. Dragic T, Litwin V, Allaway GP, Martin SR, Huang Y, et al. (1996) HIV-1 entry into CD4+ cells is mediated by the chemokine receptor CC-CKR-5. Nature 381: 667–673.
16. Feng Y, Broder CC, Kennedy PE, Berger EA (1996) HIV-1 entry cofactor: functional cDNA cloning of a seven-transmembrane, G protein-coupled receptor. Science 272: 872–877.
17. Gorry PR, Ancuta P (2011) Coreceptors and HIV-1 pathogenesis. Curr HIV/AIDS Rep 8: 45–53.
18. Peters PJ, Duenas-Decamp MJ, Sullivan WM, Clapham PR (2007) Variation of macrophage tropism among HIV-1 R5 envelopes in brain and other tissues. J Neuroimmune Pharmacol 2: 32–41.
19. Koyanagi Y, Miles S, Mitsuyasu RT, Merrill JE, Vinters HV, et al. (1987) Dual infection of the central nervous system by AIDS viruses with distinct cellular tropisms. Science 236: 819–822.
20. Cashin K, Roche M, Sterjovski J, Ellett A, Gray LR, et al. (2011) Alternative coreceptor requirements for efficient CCR5- and CXCR4-mediated HIV-1 entry into macrophages. J Virol 85: 10699–10709.
21. Lapham CK, Zaitseva MB, Lee S, Romanstseva T, Golding H (1999) Fusion of monocytes and macrophages with HIV-1 correlates with biochemical properties of CXCR4 and CCR5. Nat Med 5: 303–308.
22. Tokunaga K, Greenberg ML, Morse MA, Cumming RI, Lyerly HK, et al. (2001) Molecular basis for cell tropism of CXCR4-dependent human immunodeficiency virus type 1 isolates. J Virol 75: 6776–6785.
23. Gruber A, Kan-Mitchell J, Kuhen KL, Mukai T, Wong-Staal F (2000) Dendritic cells transduced by multiply deleted HIV-1 vectors exhibit normal phenotypes and functions and elicit an HIV-specific cytotoxic T-lymphocyte response in vitro. Blood 96: 1327–1333.
24. Tan PH, Beutelspacher SC, Xue SA, Wang YH, Mitchell P, et al. (2005) Modulation of human dendritic-cell function following transduction with viral vectors: implications for gene therapy. Blood 105: 3824–3832.
25. Kaushik R, Zhu X, Stranska R, Wu Y, Stevenson M (2009) A cellular restriction dictates the permissivity of nondividing monocytes/macrophages to lentivirus and gammaretrovirus infection. Cell Host Microbe 6: 68–80.
26. Negre D, Mangeot PE, Duisit G, Blanchard S, Vidalain PO, et al. (2000) Characterization of novel safe lentiviral vectors derived from simian immunodeficiency virus (SIVmac251) that efficiently transduce mature human dendritic cells. Gene Ther 7: 1613–1623.
27. Goujon C, Jarrosson-Wuilleme L, Bernaud J, Rigal D, Darlix JL, et al. (2006) With a little help from a friend: increasing HIV transduction of monocyte-derived dendritic cells with virion-like particles of SIV(MAC). Gene Ther 13: 991–994.
28. Goujon C, Arfi V, Pertel T, Luban J, Lienard J, et al. (2008) Characterization of simian immunodeficiency virus SIVSM/human immunodeficiency virus type 2 Vpx function in human myeloid cells. J Virol 82: 12335–12345.
29. Goujon C, Riviere L, Jarrosson-Wuilleme L, Bernaud J, Rigal D, et al. (2007) SIVSM/HIV-2 Vpx proteins promote retroviral escape from a proteasome-dependent restriction pathway present in human dendritic cells. Retrovirology 4: 2.
30. Hrecka K, Hao C, Gierszewska M, Swanson SK, Kesik-Brodacka M, et al. (2011) Vpx relieves inhibition of HIV-1 infection of macrophages mediated by the SAMHD1 protein. Nature 474: 658–661.
31. Laguette N, Sobhian B, Casartelli N, Ringeard M, Chable-Bessia C, et al. (2011) SAMHD1 is the dendritic- and myeloid-cell-specific HIV-1 restriction factor counteracted by Vpx. Nature 474: 654–657.
32. Baldauf HM, Pan X, Erikson E, Schmidt S, Daddacha W, et al. (2012) SAMHD1 restricts HIV-1 infection in resting CD4(+) T cells. Nat Med 18: 1682–1687.
33. Goldstone DC, Ennis-Adeniran V, Hedden JJ, Groom HC, Rice GI, et al. (2011) HIV-1 restriction factor SAMHD1 is a deoxynucleoside triphosphate triphosphohydrolase. Nature 480: 379–382.
34. Kim B, Nguyen LA, Daddacha W, Hollenbaugh JA (2012) Tight interplay among SAMHD1 protein level, cellular dNTP levels, and HIV-1 proviral DNA synthesis kinetics in human primary monocyte-derived macrophages. J Biol Chem 287: 21570–21574.
35. Bergamini A, Perno CF, Dini L, Capozzi M, Pesce CD, et al. (1994) Macrophage colony-stimulating factor enhances the susceptibility of macrophages to infection by human immunodeficiency virus and reduces the activity of compounds that inhibit virus binding. Blood 84: 3405–3412.
36. Kedzierska K, Maerz A, Warby T, Jaworowski A, Chan H, et al. (2000) Granulocyte-macrophage colony-stimulating factor inhibits HIV-1 replication in monocyte-derived macrophages. AIDS 14: 1739–1748.
37. Matsuda S, Akagawa K, Honda M, Yokota Y, Takebe Y, et al. (1995) Suppression of HIV replication in human monocyte-derived macrophages induced by granulocyte/macrophage colony-stimulating factor. AIDS Res Hum Retroviruses 11: 1031–1038.
38. Pauls E, Jimenez E, Ruiz A, Permanyer M, Ballana E, et al. (2013) Restriction of HIV-1 replication in primary macrophages by IL-12 and IL-18 through the upregulation of SAMHD1. J Immunol 190: 4736–4741.
39. Berger A, Sommer AF, Zwarg J, Hamdorf M, Welzel K, et al. (2011) SAMHD1-deficient CD14+ cells from individuals with Aicardi-Goutieres syndrome are highly susceptible to HIV-1 infection. PLoS Pathog 7: e1002425.
40. Cribier A, Descours B, Valadao AL, Laguette N, Benkirane M (2013) Phosphorylation of SAMHD1 by cyclin A2/CDK1 regulates its restriction activity toward HIV-1. Cell Rep 3: 1036–1043.
41. White TE, Brandariz-Nunez A, Valle-Casuso JC, Amie S, Nguyen LA, et al. (2013) The retroviral restriction ability of SAMHD1, but not its deoxynucleotide triphosphohydrolase activity, is regulated by phosphorylation. Cell Host Microbe 13: 441–451.
42. Welbourn S, Dutta SM, Semmes OJ, Strebel K (2013) Restriction of virus infection but not catalytic dNTPase activity is regulated by phosphorylation of SAMHD1. J Virol 87: 11516–11524.
43. Diget EA, Zuwala K, Berg RK, Laursen RR, Soby S, et al. (2013) Characterization of HIV-1 infection and innate sensing in different types of primary human monocyte-derived macrophages. Mediators Inflamm 2013: 208412.
44. Cheng-Mayer C, Rutka JT, Rosenblum ML, McHugh T, Stites DP, et al. (1987) Human immunodeficiency virus can productively infect cultured human glial cells. Proc Natl Acad Sci U S A 84: 3526–3530.
45. Ghafouri M, Amini S, Khalili K, Sawaya BE (2006) HIV-1 associated dementia: symptoms and causes. Retrovirology 3: 28.
46. Nomaguchi M, Doi N, Fujiwara S, Saito A, Akari H, et al. (2013) Systemic biological analysis of the mutations in two distinct HIV-1mt genomes occurred during replication in macaque cells. Microbes Infect 15: 319–328.

OPEN ACCESS Freely available online

PLOS | ONE

Slower Uncoating Is Associated with Impaired Replicative Capability of Simian-Tropic HIV-1

Ken Kono[1¤☯], Eri Takeda[1☯], Hiromi Tsutsui[1], Ayumu Kuroishi[1], Amy E. Hulme[2], Thomas J. Hope[2], Emi E. Nakayama[1], Tatsuo Shioda[1*]

1 Department of Viral Infections, Research Institute for Microbial Diseases, Osaka University, Suita, Osaka, Japan, **2** Department of Cell and Molecular Biology, Feinberg School of Medicine, Northwestern University, Chicago, Illinois, United States of America

Abstract

Human immunodeficiency virus type 1 (HIV-1) productively infects only humans and chimpanzees, but not Old World monkeys, such as rhesus and cynomolgus (CM) monkeys. To establish a monkey model of HIV-1/AIDS, several HIV-1 derivatives have been constructed. We previously generated a simian-tropic HIV-1 that replicates efficiently in CM cells. This virus encodes a capsid protein (CA) with SIVmac239-derived loops between α-helices 4 and 5 (L4/5) and between α-helices 6 and 7 (L6/7), along with the entire *vif* from SIVmac239 (NL-4/5S6/7SvifS). These SIVmac239-derived sequences were expected to protect the virus from HIV-1 restriction factors in monkey cells. However, the replicative capability of NL-4/5S6/7SvifS in human cells was severely impaired. By long-term cultivation of human CEM-SS cells infected with NL-4/5S6/7SvifS, we succeeded in partially rescuing the impaired replicative capability of the virus in human cells. This adapted virus encoded a G-to-E substitution at the 116th position of the CA (NL-4/5SG116E6/7SvifS). In the work described here, we explored the mechanism by which the replicative capability of NL-4/5S6/7SvifS was impaired in human cells. Quantitative analysis (by real-time PCR) of viral DNA synthesis from infected cells revealed that NL-4/5S6/7SvifS had a major defect in nuclear entry. Mutations in CA are known to affect viral core stability and result in deleterious effects in HIV-1 infection; therefore, we measured the kinetics of uncoating of these viruses. The uncoating of NL-4/5S6/7SvifS was significantly slower than that of wild type HIV-1 (WT), whereas the uncoating of NL-4/5SG116E6/7SvifS was similar to that of WT. Our results suggested that the lower replicative capability of NL-4/5S6/7SvifS in human cells was, at least in part, due to the slower uncoating of this virus.

Citation: Kono K, Takeda E, Tsutsui H, Kuroishi A, Hulme AE, et al. (2013) Slower Uncoating Is Associated with Impaired Replicative Capability of Simian-Tropic HIV-1. PLoS ONE 8(8): e72531. doi:10.1371/journal.pone.0072531

Editor: Zhiwei Chen, The University of Hong Kong, Hong Kong

Received April 19, 2013; **Accepted** July 10, 2013; **Published** August 13, 2013

Funding: This work was supported by the Japan Society for the Promotion of Science Excellent Young Researcher Overseas Visit Program and grants from the Ministry of Education, Culture, Sports, Science, and Technology; the Ministry of Health, Labour and Welfare, Japan; and the Health Science Foundation. This work also was supported by NIH grants RO1 AI47770 and P50 GM082545 to TJH and F32AI089359 to AEH. The funders had no role in study design, data collection and analysis, decision to publish, or preparation of the manuscript.

Competing interests: The authors have declared that no competing interests exist.

* E-mail: shioda@biken.osaka-u.ac.jp

☯ These authors contributed equally to this work.

¤ Current address: Division of Medical Devices, National Institute of Health Sciences, Tokyo, Japan

Introduction

HIV-1 infection begins with the interaction and fusion of viral and cellular membranes. After fusion, a conical core, consisting of the two viral genomic RNAs and several viral proteins, is released into the cytoplasm of the target cell. The major component of the core is the viral capsid protein (CA). In the cytoplasm, CA eventually dissociates from the viral complex in a process termed uncoating. During this time, reverse transcription (RT) of the viral genomes occurs. The resultant double-stranded DNA associates with viral and cellular proteins, constituting the pre-integration complex (PIC). The PIC migrates into the nucleus, where the viral DNA integrates into the chromosomal DNA of the target cell.

HIV-1 uncoating was thought to occur immediately following viral fusion, as CA was undetectable in RT complexes isolated from infected cells [1–3]. Thus, CA was thought to have only a minor role in HIV-1 infection. However, subsequent reports indicated that mutations in CA decreased HIV-1 infectivity. Most of these CA mutant viruses displayed decreased levels of RT products [4–10]. On the other hand, the mutant virus Q63/67A, which encodes two Gln-to-Ala substitutions in CA, exhibited a defect in nuclear entry [4,11,12]. Changes in core stability caused by some of these CA mutations seem to affect uncoating kinetics, which may result in impaired RT or nuclear